COMPUTER MODELING OF HEAT PUMPS
AND THE
SIMULATION OF SOLAR ENERGY-HEAT PUMP SYSTEMS

BY

THOMAS LEE FREEMAN

A thesis submitted in partial fulfillment of the requirements for the degree of

MASTER OF SCIENCE
(Engineering)

at the

UNIVERSITY OF WISCONSIN-MADISON

1975

ACKNOWLEDGMENT

I am very grateful for the encouragement and guidance of my advisors, Professors W. A. Beckman and J. A. Duffie. The helpful suggestions of Professors J. W. Mitchell and E. P. Mikol have been greatly appreciated. I also wish to acknowledge the countless ideas and technical contributions from my fellow graduate students at the University of Wisconsin Solar Energy Laboratory, namely, Dennis Beekman, Vernon Karman, Mike Eberlein, Sanford Klein, Pat Hughes and Rodney Oonk.

I thank my parents for their support during this work and especially my mother for typing the manuscript. Special thanks are extended for the patience and faithfulness of my trusty dog, Jesse. Finally, the financial assistance of the National Science Foundation under grant NSF/RANN/GI34029 is gratefully acknowledged.

COMPUTER MODELING OF HEAT PUMPS AND THE SIMULATION OF SOLAR ENERGY-HEAT PUMP SYSTEMS

TABLE OF CONTENTS

LIST OF FIGURES

LIST OF TABLES

LIST OF APPENDIX

1.0 INTRODUCTION

1.1 BACKGROUND

A heating and cooling system combining a heat pump and a solar energy system has a number of attractive features. Alone, each is economically marginal in many parts of the nation today. Together, they may be able to compensate for some of each other's shortcomings.

Since moderate temperature heat source reservoirs (like lake or ground water) are not generally available, most heat pump systems are forced to rely on ambient air as a heat source in the heating mode. At low ambient temperatures the air source heat pump's coefficient of performance, COP (the ratio of delivered energy to input electrical energy) drops rapidly toward unity. For ambient temperatures under 0° C, moisture in the outdoor air condenses and freezes on the evaporator coil requiring that the heat pump be switched to the cooling mode periodically to defrost the coils. The resultant waste of energy may reduce the average COP below unity. From the point of view of the utilities, widespread utilization of heat pumps may cause unacceptable peak loading on very cold and very hot days. As for solar energy systems working alone, the obvious shortcoming of most systems is their lack of space cooling capability, and at acceptable efficiencies, the outlet temperatures of inexpensive collectors are often below the lower limit of usefulness for space heating.

performance. The transient nature of solar energy system performance requires that consideration be made of the transient effects, but many authors model the weather, the solar collection system, and the heat pump all on the basis of some kind of "mean". The results so obtained may be valid for steady state operation over a relatively short time when the mean conditions prevail, but it is unlikely that these results can be interpreted as long-term averages.

Jordan and Threlkeld (1) have written a series of papers investigating the feasibility of solar heat pump systems. They conclude from a thermodynamic analysis that multiple step condensation is optimal for heat pump applications in solar systems. From manufacturers ratings and their own analysis they are able to derive a semi-empirical relation for COP for their proposed designs. Their performance studies are based on a constant condensing and evaporating temperature, a "typical" January mid-day solar radiation level, and a constant collector efficiency. The authors conclude that evaporator side storage is clearly superior. Their economic analysis suggests that the solar-heat pump systems have low feasibility in the northern United States but relatively high feasibility in the south.

Lof (2) did another feasibility study, limited to systems employing evaporator side storage, a heat pump that uses either the solar storage tank or outdoor air as a source when storage is depleted, and electrical resistance auxiliary. The average

Calvert and Harden (5) perform an economic analysis for heating and cooling a specific residence in Tulsa, Oklahoma, with several different kinds of appliances supplying heat and air conditioning. After concluding that the electric heat pump is a viable alternative, they investigate providing the heat pump with a solar energy source to increase its capacity and reduce the substantial electric resistance heat required. Assuming a constant COP, a constant source (storage) temperature, a constant collector efficiency, and an average solar energy flux, they estimate the collector and storage size requirements for this residence and climate.

Bridges, Paxton, and Haines (6) discuss many of the practical considerations in the design, operation, and maintenance of their solar energy heat pump office building in Albuquerque, New Mexico. They present a comparison of recorded performance for a heating season to predicted performance calculated from a simplified model. Loads were found from the degree-day method. Daily average ambient temperatures were taken from weather bureau records as was incident solar energy which was subsequently corrected for collector tilt by a multiplicative factor of 2.3 on "sunny" days and 1.0 on "cloudy" days. Collector efficiencies were calculated as a function of storage and ambient temperatures on a daily basis. No attempt was made to model the heat pump performance other than to assume that, on the average, the system withdrew .8 of the heating load from storage (equivalent to assuming an

There are a number of possible solar energy-heat pump system configurations described in the literature, e.g., Bridges et al. (6), Yanagimachi (10), and Jardine (11). These systems have several different modes of providing heating or cooling to the load, depending on availability and demand. The systems and modes can be separated into two general classes of configurations: "in-line" systems where the heat pump is located between the solar collection loop and the heat load loop, and "parallel" systems where the heat pump can add (or remove) heat from the load independently of the solar system operation. The second objective of this paper is to compare these two different system configurations and perform a cursory economic evaluation.

methods by which the user would supply the program with heat exchanger surface geometry, heat transfer characteristics or compressor construction details, for example. It would be difficult to "design" a machine of a desired capacity in this way, and only an experienced or lucky designer would end up with a heat pump with typical performance characteristics.

The model should be as flexible as possible in order to represent a large variety of designs. Both heating and cooling must be considered, of course. The user should have the option of switching modes by altering the refrigerant flow path or diverting the hot and cold side flowstreams. These flowstreams may be either gas or liquid so the model should be able to handle either. The model should not be limited to a particular refrigerant.

The solar energy system designer, just like the heating and ventilating engineer, is going to want to deal with heat pumps of known capacity at known (i.e., rated) conditions. For this reason, the model should be able to produce "typical" characteristics that include a "rated" output at the "rated" conditions supplied by the user.

Solar heating and cooling systems involving heat pumps must be simulated for relatively long periods of time, due in part to the differing demands on the system as the seasons change. TRNSYS simulations usually require a computational time step of no more than one hour. Thus it becomes critical additional comments on the design procedure are in order.

The emphasis of this heat pump modeling method is not so much to design a particular piece of hardware with high accuracy, but rather to see how a typical machine that is designed to deliver a specified output at specified conditions will operate off design conditions. For this reason, it is not highly critical to have precise design condition values for such parameters as condensing and evaporating heat transfer coefficients (which are almost impossible to obtain analytically). What is important to this model is knowledge of the way in which the design condition parameters change when the heat pump is operating off its design point (e.g., the functional relationship of heat transfer coefficients to refrigerant flow rate). During the development of the program it has been observed that when a specific rated output is sought, substantial changes to many design parameters and assumptions result only in the design of a different piece of hardware (e.g., larger or smaller heat exchangers). The way in which these different designs operate off rated conditions is often not too different. For this reason, it has been found unnecessary to define a piece of hardware with great detail. A relatively few pieces of information sufficiently characterize a heat pump for the purposes of this model.

and much of the time, the heat pump is being called with inputs for which outputs have already been found. Thus a great computational savings can be realized by creating a performance map.

A performance map is a set of solutions or operating points corresponding to a set of possible combinations of input variables. Maps are constructed by repeatedly solving for the rates of heat addition and heat rejection as all the inputs are stepped through small intervals within their ranges. These maps become matrixes from which an interpolation routine obtains performance data at finite intervals and interpolates between for the heat pump solution at any set of inputs within the map's range. To limit the amount of mapping required, the flow rates of the exchange fluids are assumed to be a constant (when turned on) for a particular map. This reduces the number of inputs to two (evaporator inlet temperature and condenser inlet temperature). The performance maps are thus two two-dimensional matrixes: (QA(I,J)) for the heat addition, and (QR(I,J)) for the heat rejection, which contain solutions for inputs (I,J) that correspond to combinations of evaporator and condenser exchange fluid inlet temperatures. Compressor work required and COP can easily be derived from this information. A more complete description of the mechanics of performance mapping and interpolation is given in Section 2.4.

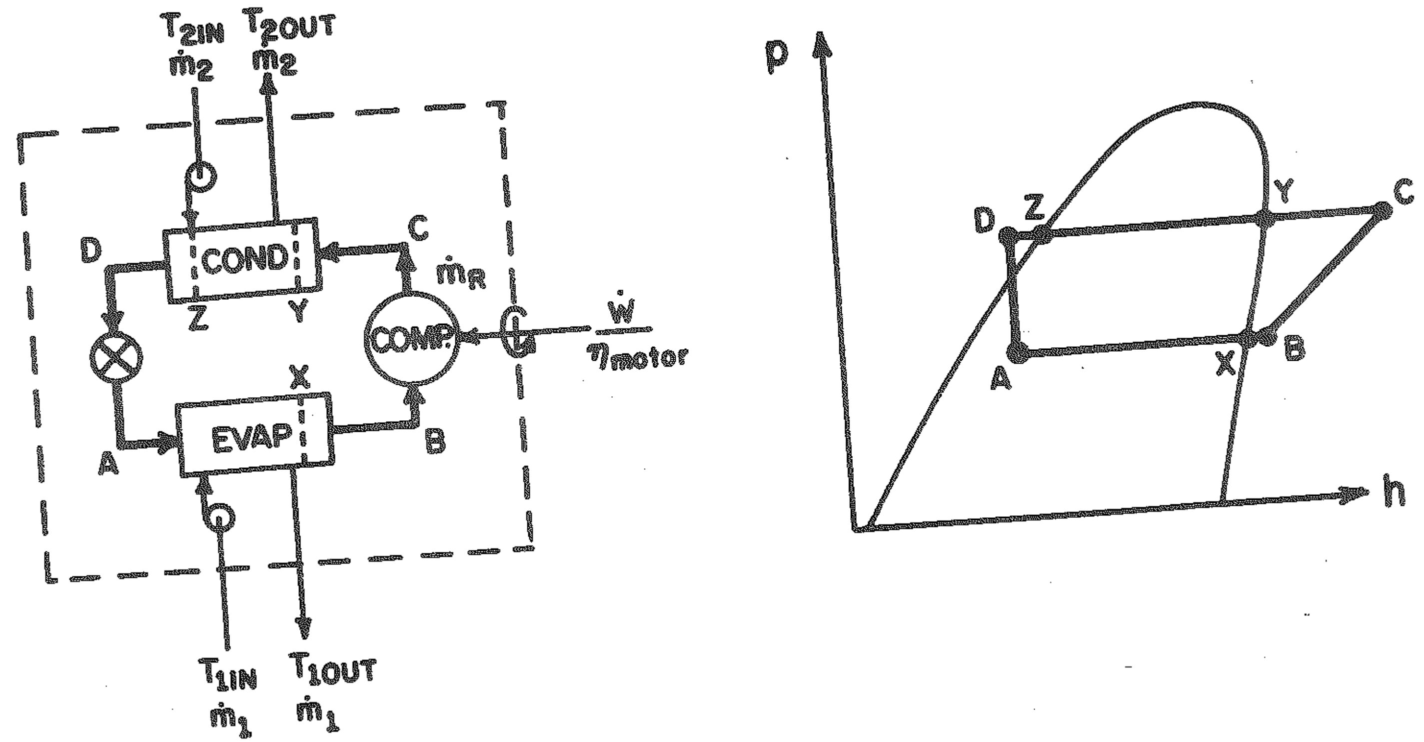

FIG. 2.1 SYSTEM SCHEMATIC AND PROCESS IN p-h PLANE

another performance map for the heat pump in the opposite mode. On the other hand, the performance map generated with this approach is usually not very accurate for real hardware in the mode for which it was not sized. This unfortunate situation is a result of shortcomings in the modeling strategy but also because the real system's heat transfer coefficients change in some nebulous way in the diverted flow situation, design condition heat exchanger ΔT's (between refrigerant and exchange fluid) differ in some unknown way, and a different expansion device is often switched into the refrigerant circuit since more restrictive flow is needed in the cooling mode.

The approach taken, therefore, is to size a "different" device for both modes of operation of the diverted refrigerant type of heat pump. It is up to the user to specify heating and cooling rated conditions (as well as other parameters) that are consistent with each other when specifying the heating and cooling modes of the same heat pump. A measure of his success in doing this is that the sizing information (printed out at the user's option) reveals that the same hardware was "designed" to meet the rated conditions in both modes.

From a practical point of view, this approach has other merits. First, the user is able to force the model to have both heating and cooling performance which agree with a real to the simple cycle reasonably well since the user has the freedom to select many parameters that affect performance but are not published by the manufacturers (e.g., compression efficiency and heat transfer coefficients). In other words, if representation of some real equipment's performance is desired, parameters can be selected for the simple single stage cycle that result in very similar characteristics.

A separate subcooler heat exchanger was originally included in the model but for small amounts of subcooling, the effect on performance was negligible. This is not to say that subcooling is undesirable, but, if exchange fluid flow must be taken away from the condenser to be added to the subcooler, the capacity gained by subcooling is very nearly lost by a reduced condenser capacity. This is the situation encountered when attempting to duplicate a real heat pump's performance curve. The manufacturer normally specifies the condenser (plus subcooler, if any), air (or water) flow rate, but not how it is divided up between the condenser and the subcooler. Nearly identical results are obtained when a condenser employing no subcooling is compared to one employing $10^{o}C$ subcooling and the same flow rate split between the condenser and the subcooler.

A more serious limitation may be the inability of the model to solve for the operating points of cycles using a capillary tube expansion device. The thermostatic expansion valve is probably the most practical device for systems at the same exchange fluid inlet temperatures for a few time constants (on the order of a minute). Therefore, the model cannot be expected to accurately represent systems whose temperatures fluctuate rapidly or which undergo frequent shut-down and start-up, where transients are especially long.

Real heat pump hardware, especially the "split" air to air systems, employ long runs of refrigerant piping from the outdoor unit to the indoor unit and back again. Pressure drop and heat transfer along these pipes are not considered in this model. For high capacity (high outdoor temperature and large refrigerant flow rate), the big pressure drops in the lines would hurt system capacity, and at low capacities (cold outdoor temperatures), the heat loss from the pipes would again hurt capacity. But, as explained previously, uniform reduction of capacity at all outdoor temperatures simply results in the sizing of a bigger (albeit more expensive) heat pump that performs about the same at all temperatures as the unpenalized smaller one.

2.2.4 CONTROL STRATEGY

In simulation of heating and cooling systems, experience has shown that there are two basic ways in which systems can be controlled. If the function of a heat pump (or furnace, air conditioner, etc.) is to meet but not exceed a calculated load, it is convenient to control on energy rates. For pump). For this reason, the on-off control function, γ_i, was added. When $\gamma_i = 0$, the heat pump is off. The heat pump exchange fluid pumps are assumed to be within the heat pump, so whenever the heat pump is off, the flow rates $\dot{m}_{1out}$ and $\dot{m}_{2out}$ are set to 0, and T_{1out} and T_{2out} are equated to T_{1in} and T_{2in}, respectively.

As discussed in the section on mode changing, no control mechanism has been developed to change the heat pump function from heating to cooling. A load model with very large dead-bands, or accurate consideration of capacitance, is a pre-requisite for automatic mode switching. Otherwise there would be unwarranted switching from daytime cooling to nighttime heating for much of the cooling season. In place of mode control in this study, the heating mode will be simulated independently of the cooling mode by isolating a "heating" season and a "cooling" season and running two separate simulations.

2.3 COMPONENT MODELING

Of the four basic components in the vapor compression cycle, the evaporator and condenser are the most difficult to model adequately. Separate subroutines have been devoted to them since these models are more involved and more subject to change than are the compressor and expansion valve models. More sophisticated and/or accurate methods of describing the heat exchangers could be developed at a later prevent "slugging", or passing of liquid droplets into the compressor, provision is made for a small amount of superheating of refrigerant vapor before it leaves the evaporator. This superheating cannot be excessive since the specific volume of the vapor decreases as the vapor is heated at constant pressure, thus decreasing the compressor's refrigerant pumping rate (higher CFM/ton) and decreasing system performance. Superheating is held to a practical minimum of about 5 - 10°C especially in thermostatic expansion valve systems where the level is maintained very nearly constant. Thus the amount of heat exchanged between the exchange fluid and boiling refrigerant is vastly greater than the heat transferred in superheating the refrigerant. Referring to the p-h diagrams of R-22 and 11, the ratio of heat transferred to superheated vapor to the total heat transferred ($\Delta h_{SH}/\Delta h_{TOT}$) for 10°C superheating is approximately 1:30 and 1:20, respectively. It will be shown that as a result of this situation, the heat exchange process in the evaporator may be approximated as heat transfer to refrigerant entirely in the two-phase region.

Although the evaporator is a single piece of heat exchange hardware, mathematically it is two heat exchangers coupled together in some, not necessarily simple, manner. For any flow arrangement other than parallel flow, a rigorous analytical solution of two coupled heat exchanger problems becomes very difficult. A series combination of parallel-

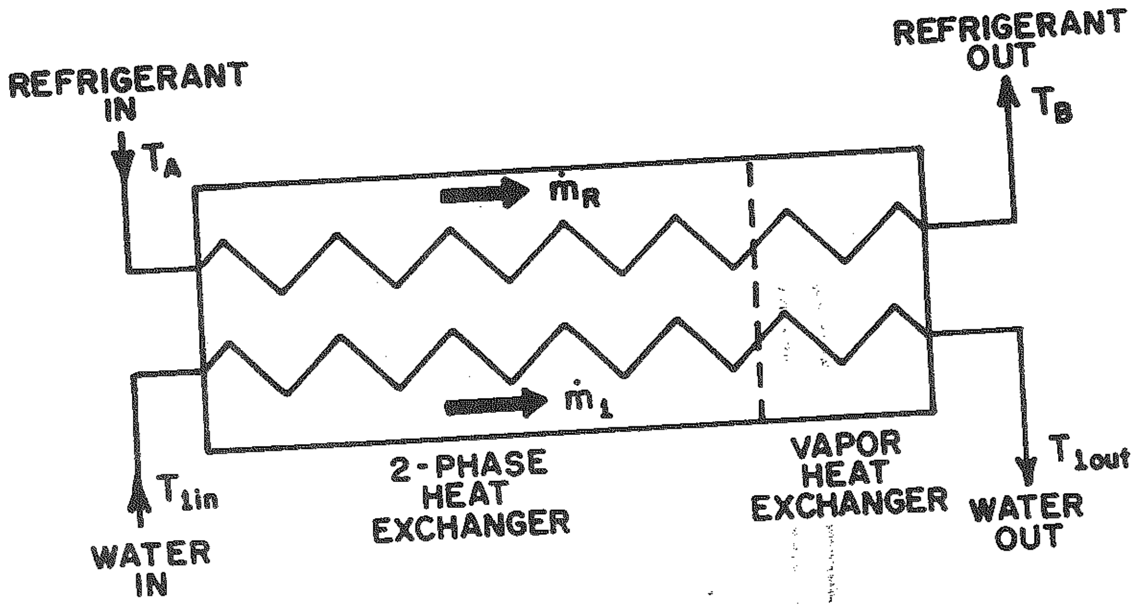

FIG. 2.2 PARALLEL FLOW EVAPORATOR MODEL

U_{EVAPdc} and A_{EVAP} referenced to the refrigerant side; $U_{EVAPdc} = 1/(1/h_{BOILdc}) + 1/h_1\ A_{REVAP}))$ neglecting wall resistance. $A_{EVAP} = UA_{dc}/U_{EVAPdc}$ and is a constant. It bears repeating at this point that the purpose of this model is not to accurately design a particular piece of hardware to meet some specifications but to characterize the way in which a "typical" machine's performance changes when operating off design conditions. For this reason, U and A have been calculated in a very straightforward way. What is of primary importance is the way in which U changes, for this is going to have a strong influence on the off design heat transfer characteristics and thus on the off design system performance.

2.3.1.3 EVAPORATOR HEAT TRANSFER COEFFICIENTS

In this model the assumption has been made of a constant exchange fluid mass flow rate. Actually this is not quite accurate since, for air systems, the fan maintains a constant volume flow rate (CFM). The air volume is proportional to absolute temperature so outdoor air entering the evaporator in the winter can undergo a sizable change in mass flow. Of course the other transport properties of air (ρ, c_p, k) also undergo changes with air temperature. However, the air side heat transfer coefficient as a function of transport properties derived in Appendix A1.1, $h_{air} = \frac{c_p^{.333}\ k^{.667}}{\mu^{.267}}\ \dot{m}_1^{.6}$, therefore: $$h_{BOIL} = \frac{T_{1in} - T_A}{T_{1indc} - T_{Adc}} h_{BOILdc}$$

This relation, though crude, is probably as good a general rule as can be found. As the refrigerant flow rate increases, the operating point temperature difference $(T_{1in} - T_A)$ will rise, resulting in an increased boiling heat transfer coefficient, so functional dependence of h_{BOIL} on flow rate is implicit in this relation.

The purpose of the evaporator model, subroutine BOILER (listed in Appendix A2.6) is to determine the refrigerant outlet state (state B) for any combination of refrigerant inlet conditions (state A) and flow rate, and exchange fluid inlet temperature. Each time called, subroutine BOILER recalculates a new off-design boiling heat transfer coefficient, h_{BOIL}, and the new over-all U value from $U_{EVAP} = 1/(1/h_{BOIL} + 1/h_1\ A_{REVAP})$. The $\epsilon - N_{tu}$ equations are then solved for QA, and h_B and T_{1out} are easily found.

2.3.1.4 EVAPORATOR FROST

An additional consideration for air-source evaporators is the possibility of frost build-up which can occur when the surfaces are below $0^{o}C$ and the air dew point is above the surface temperature. Frost is detrimental to the operation of the system for three reasons. A layer of frost build-up adds additional heat transfer resistance to the evaporator resulting in a smaller U. The frost increases

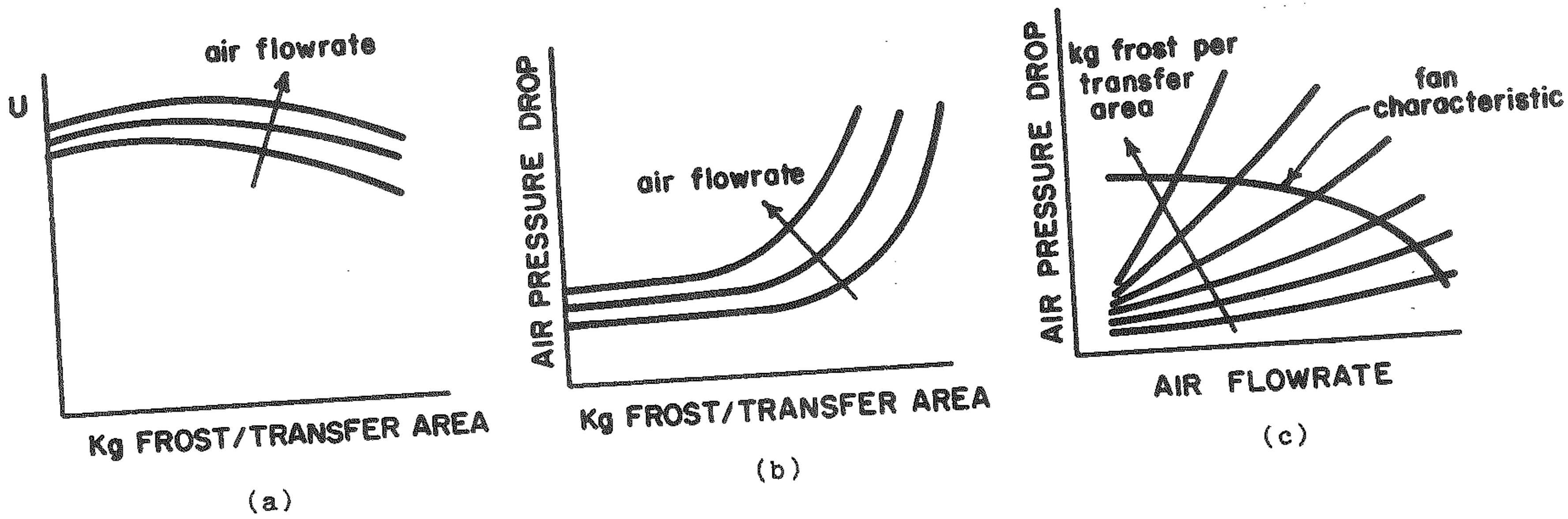

FIG. 2.3 THE EFFECTS OF FROST FORMATION ON COIL PERFORMANCE

for both refrigerants. The use of a single two-phase heat exchanger to represent this significant amount of heat transferred from superheated vapor would seem unacceptable. However, the exact solution of two coupled heat exchangers for any case but the parallel flow configuration is so difficult that some simplifications must be made.

Fig. 2.4 shows the most common fin-tube flow arrangements where air (or any gas) is the exchange fluid. A number of shell and tube flow arrangements where water (or any liquid) is the exchange fluid are shown in Fig. 2.5.

2.3.2.1 AIR SOURCE CONDENSER

Characterization of the two coupled heat exchangers in terms of known heat exchanger flow arrangement solutions is much more straightforward with the air (cross-flow) configuration. The way in which the equations are linked is minimal since the air through the superheat heat exchanger is separate from the air which flows through the two-phase heat exchanger for almost any conceivable flow tube geometry. The state of the refrigerant as it enters the two-phase heat exchanger is simply the exit state of the superheat heat exchanger (state Y). The location of state Y is free to move as conditions change. Fig. 2.6a shows the cross flow condenser from the air flow direction and illustrates how the two heat exchanger problems are quite separate no matter what the tube geometry. Fig. 2.6b shows how the cross flow condenser

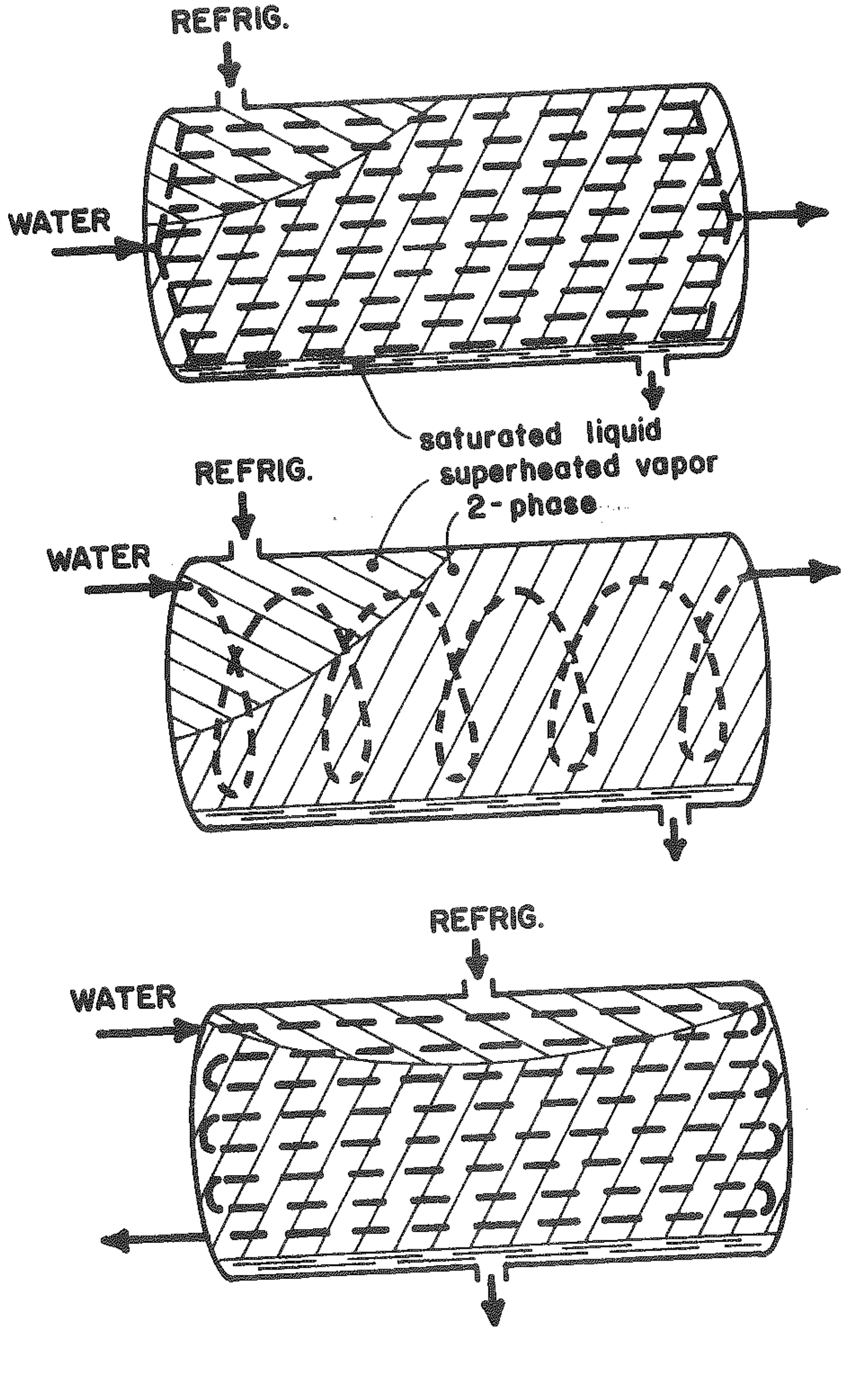

FIG. 2.5 TUBE-SHELL FLOW ARRANGEMENTS

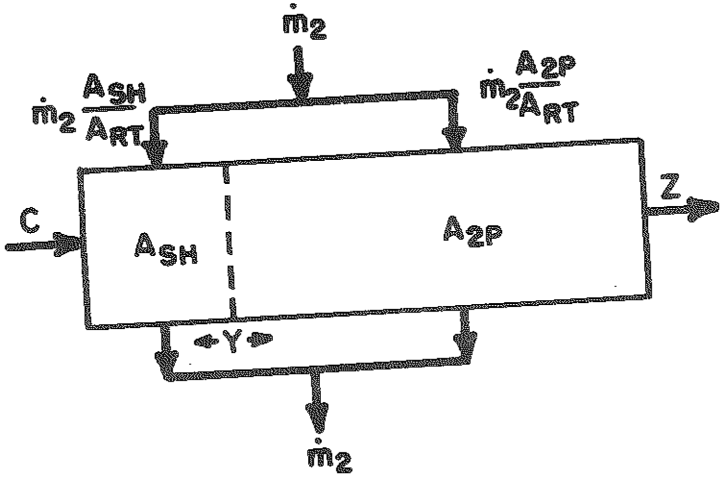

(b)

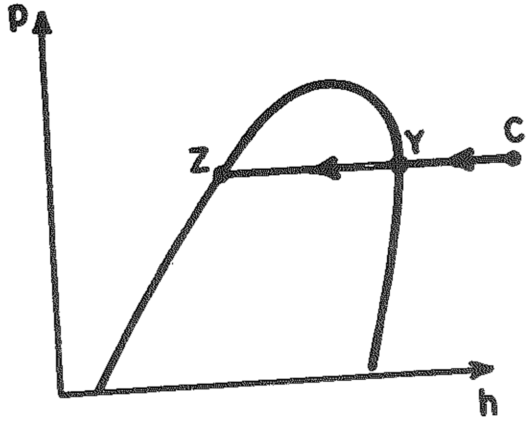

(c)

FIG. 2.6 CROSSFLOW CONDENSER (cont.)

2.3.2.2 WATER SOURCE CONDENSER

From the experience gained in modeling the cross flow condenser, it was decided that some simplification was both necessary and justifiable for the liquid cooled condenser. The liquid cooled (or water source) condenser cannot be separated into two distinct heat exchangers for which simple analytical solutions exist. A fluid may repeatedly pass into and out of both heat exchangers (e.g., the water in Fig. 2.5). Clearly, a simplified model is required. One can imagine a hypothetical flow arrangement consisting of two separated parallel-counter flow heat exchangers which is easy to solve (though impossible to build). The key assumption here is that a separate parallel-counter flow heat exchanger is available to de-superheat the refrigerant vapor and yet all of the refrigerant and all of the liquid flow through both heat exchangers, thus eliminating the need for an iterative sizing algorithm as required in the cross flow analysis. Again, the flow arrangement in the two-phase heat exchanger does not affect the heat exchanger equations.

From the same information available in the cross-flow analysis, the sizing routine must find the design condition UA's, U's and A's. This process (described in Appendix A1.3) is relatively straightforward, requiring the solution of the separated $\epsilon - N_{tu}$ equations for UA in terms of known heat and mass flow quantities.

does include, is the strong dependence of the heat transfer coefficient on the mass flow rate (per unit area) of the refrigerant (G). Accordingly, for refrigerant flow inside tubes, h_{RSH} is re-computed every time the condenser subroutine is called by scaling h_{RSHdc} by the factor $(\dot{m}_R/\dot{m}_{Rdc})^{0.8}$. In liquid cooled condensers, the refrigerant condenses on outer tube walls. The vaporized refrigerant heat transfer coefficient is less dependent on flow rate in this circumstance and h_{RSH} is taken to be $h_{RSHdc}(\dot{m}_R/\dot{m}_{Rdc})^{0.5}$.

The condenser heat transfer coefficient of primary importance is the condensing coefficient, h_{R2P}, but it is also the most difficult to evaluate. For film condensation outside horizontal tubes, Nusselt proposed:

$$h_o = .725\left(\frac{k_f^3\,\rho_f(\rho_f-\rho_v)\;gh_{fg}}{N\;D\,\mu_f\Delta t}\right)^{1/4}$$

When evaluated over a wide range of condensing temperatures, this equation gives variations of 30% for R-22 and about 15% for R-11. Nevertheless, for the following reasons it was decided to leave h_{R2P} constant at its design condition value, h_{R2Pdc}. This model is not sufficiently detailed to discern between film and dropwise condensation (which would modify the Nusselt equation considerably). For condensation inside tubes (the situation for air cooled condensers), Nusselt's correlation must be modified again to account for the fact that decreasing amounts of surface area along the flow direction are available to vapor condensation as liquid collects refrigerant inlet state, and refrigerant flow rate, there is a pressure at which state D does occur where desired. It is one of the functions of subroutine HTPMP to iteratively find this pressure.

In conclusion of the condenser discussion, the following observations are noted. Most heat is transferred in condensers from condensing refrigerant where the mechanism is virtually the same for any flow arrangement (exactly the same as far as the $\varepsilon - N_{tu}$ equations are concerned). Therefore the differentiation made between cross-flow and parallel-counter flow arrangements affects only the small amount of heat transferred in desuperating the vapor. In retrospect, the effort expended in treating this detail is probably unwarranted. In fact, it is common practice in the refrigeration industry to treat the condenser as if all heat were transferred in two-phase (as done in the evaporator model). According to Stoecker (24), in the superheated region the effects of a smaller heat transfer coefficient are very nearly balanced by the larger Δt, justifying the simplification.

2.3.3 THE COMPRESSOR

The refrigerant mass flow rate through a reciprocating compressor is related to its displacement rate (DR), the inlet specific volume (v_{suct}), and the volumetric efficiency (η_v).

$$\dot{m}_R = (DR\ \eta_v)/v_{suct}$$

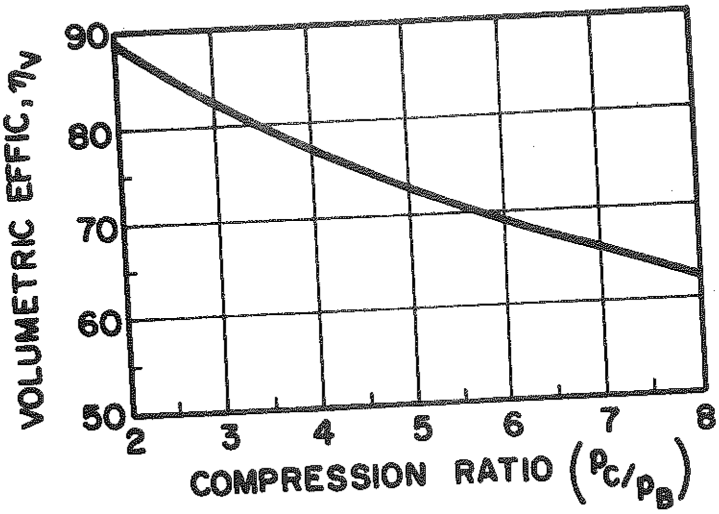

FIG. 2.7 VOLUMETRIC EFFICIENCY AS A FUNCTION OF PRESSURE RATIO (from TRANE AIR CONDITIONING MANUAL)

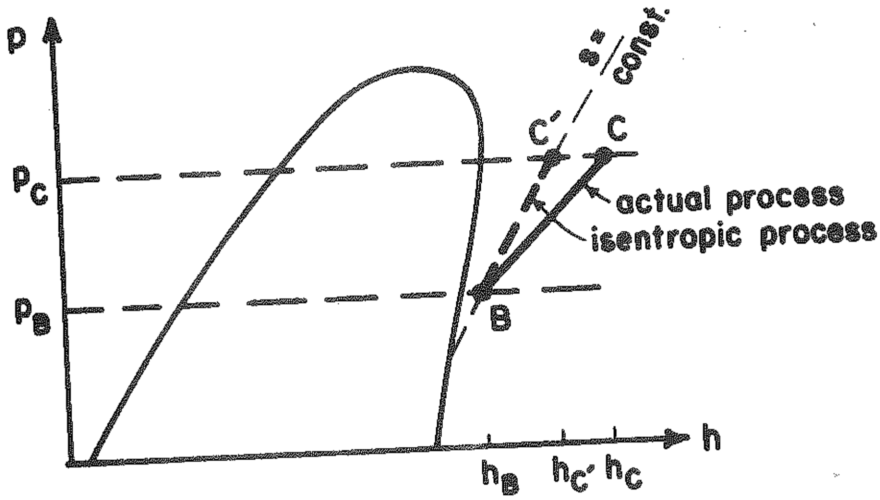

FIG. 2.8 COMPRESSION PROCESS IN p-h PLANE

that have to operate over wide ranges of hot and cold side temperatures since the valve ensures nearly optimum usage of all the evaporator heat exchange surface. This is done by throttling the refrigerant such that a small and fairly constant amount of superheating is maintained at the evaporator outlet. The thermostatic expansion valve's orifice size is regulated by three forces acting upon a diaphragm rigidly connected to the throttling pin inside the orifice. A bulb charged with refrigerant is affixed to the outlet of the evaporator so that the bulb follows the evaporator temperature. If the bulb is charged with the same refrigerant as the evaporator, the bulb pressure, P_1, will be the pressure at saturation of the superheated vapor leaving the evaporator. P_1 acts on one side of the diaphragm tending to open the valve. Balancing this force on the opposite side are the evaporator pressure, P_2, and a constant spring pressure, P_3, tending to close the valve (see Fig. 2.9).

If the valve does not feed enough refrigerant, the evaporator pressure drops and/or the bulb temperature is increased by the warmer vapor leaving the evaporator. Thus an opening force is exerted on the valve pin, admitting more refrigerant until the three pressures are again in balance. Conversely, if too much refrigerant is fed into the evaporator, the bulb temperature decreases and/or the evaporator pressure increases so that a closing force is exerted on the pin until the pressures are again in balance.

Modeling the thermostatic expansion valve is not difficult, however, since the orifice size is not of direct interest. It is sufficient to assume that the valve is capable of adjusting the opening in such a way that a constant amount of superheating is maintained. One other constraint is required to characterize the valve and that is the customary assumption of a constant enthalpy expansion process.

There is, however, one complication to add to this simple model. In practical heat pump systems operating at very high capacities, the evaporator can be "starved" by the valve's failure to pass enough refrigerant. This may happen because the valve cannot open any further or because the reservoir of liquid refrigerant in the condenser accumulator has been depleted. As the heat pump hot and cold side temperature difference becomes small, the pressure ratio approaches unity resulting in a high volumetric efficiency, a large refrigerant flow rate, and a high heat pump capacity. A limit to the increase in flow rate is reached when the valve opens its widest to pass more refrigerant but still can't keep point B on the locus of constant superheat. This condition does not occur in a good design within the normal operating range of the hardware. In most air to air heat pumps, for example, refrigerant flow is not limited by the expansion valve in the heating mode until the outdoor temperature is within approximately $5^{o}C$ of the indoor

For a given refrigerant $v_{sat\ liq}$ is essentially constant and the maximum orifice area, $A_{wide\ open}$, is a constant, so the relation reduces to:

$$\dot{m}_R = C\sqrt{\Delta p}$$

Fig. 2.10 shows conceptually how the compressor refrigerant mass flow and the expansion valve mass flow relations are simultaneously satisfied as the condensing and evaporating temperatures change. In this illustration, it is assumed that the uppermost compressor curve results when the evaporation pressure is held constant at p_{B1} and the condensing pressure is successively ~~lowered~~ so that $\Delta p = \Delta p_1$, Δp_2, Δp_3, etc. The compressor is able to pump more refrigerant as the pressure ratio approaches unity, and the thermostatic expansion valve adjusts to the new operating point by increasing the orifice area. At $\Delta p_4 = \Delta p_{lim}$, however, the valve is wide open and further decrease of condensing pressure results in a decrease of mass flow rate along the "wide open" curve. State B is no longer constrained to be on the locus of constant superheat, and the evaporator pressure is free to find a new level. The new compressor characteristic is the next lower curve and the new balance point is point 5. As $\Delta p \rightarrow 0$ there is no pressure across the expansion valve and $m_R \rightarrow 0$. These considerations will be discussed further in the description of the solution technique (Section 2.4).

The one problem remaining in the expansion valve model is how to provide a maximum orifice size criteria that the user can specify. The obvious way would be to have the user supply the constant, C. This approach, however, requires unjustifiably detailed knowledge of the hardware. The approach decided upon requires only the specification of a pressure ratio, RP_{lim}, (corresponding to p_{lim} in Fig. 2.10) under which the expansion valve is assumed to be wide open and therefore limiting the flow of refrigerant. The program uses this information to determine the value of C. This is done by equating the refrigerant mass flow rate expressions of the compressor and the expansion valve at this critical, limiting case operating point. (i.e., evaporator pressure = P_{Bdc}, condenser pressure = $P_{Clim} = RP_{lim}\, P_{Bdc}$ State B is on the locus of constant superheat.)

Then $\dot{m}_R = \dfrac{DR\,\eta_v}{v_B} = C\sqrt{P_{Clim} - P_{Bdc}}$ where $\eta_v = f(RP_{lim})$

The value of C obtained from solving this equation, it must be remembered, corresponds to the wide open valve only. Whenever $C\sqrt{\Delta p} > \dfrac{DR\,\eta_v}{v_B}$, the valve is partially closed and is maintaining constant superheat. But when $C\sqrt{\Delta p}$ tends to fall beneath $\dfrac{DR\,\eta_v}{v_B}$, the valve is limiting flow, and the constant superheat constraint is replaced in the solution criteria by the equation $C\sqrt{\Delta p} = DR\,\eta_v/v_B = \dot{m}_R$.

specified by the user. Within that range lie an infinite number of ordered pairs, T_{1in}, T_{2in}, for which an operating state exists (although the solution may be that the heat pump is off). In general, when an ordered pair T_{1in}, T_{2in} is specified, the solution subroutine HTPMP (listed in Appendix A2.3) iteratively searches for the states A, B, C and D that satisfy the component modeling equations set forth in Section 2.3.

The algorithm is a modified form of Newton's method in two dimensions. The functions for which zeroes are to be found are DELHB (P_B, P_C) and DELHZ (P_B, P_C). These functions represent the amount of "overshoot" (positive or negative) of the locus of constant superheat line that point B ultimately must lie on, and the saturated liquid line which point Z ultimately must lie on. It must be remembered that when CNDNSR and BOILER are called, they solve the heat exchanger equations and return the end states of the condensation and evaporation processes which, in general, either undershoot or overshoot the locus of permissible endstates. The iterative approach to locating these pressures is analogous to "hunting" in a real system where pressures and endstates oscillate somewhat when the inlet conditions change before the new "steady state" operating states are found. The object of the iterative Newton's method, then, is to find the combination of evaporator and condenser pressures (P_B and P_C)

to keep point B on the locus of constant superheat. In a real system, when the evaporator begins to starve, point B drifts further out into superheat, the compressor inlet specific volume goes up, and the compressor flow rate goes down, resulting in a stabilizing effect that tends to limit the evaporator starvation problem. An effort to duplicate this effect in the iterative solution technique was never entirely successful. The solution algorithm often became unstable, predicting new state B points far into superheat or pressures that diverged rapidly. It is believed that the basic concept is sound but that another method of implementation is required. At any rate, this problem only affects the heat pump solutions at very high refrigerant flow rates. Many possible expedients were investigated to enable an approximate solution in this situation. The procedure finally employed uses the following algorithm. Subroutine HTPMP solves for the operating states as usual assuming there is no refrigerant flow limitation. It then checks to see if the flow rate as calculated by a fully open valve, $C\sqrt{P_C - P_B}$, is exceeded by the flow rate as calculated by the compressor equation, $DR\,\eta_v\,/v_B$. If so, the pressure difference $(P_C - P_B)$ is iteratively increased (which increases the valve flow rate and decreases the compressor flow rate) until the two flow rates are equal. This method results in a solution that satisfies the mass flow rate constraints of the compressor and valve but does not in general satisfy the

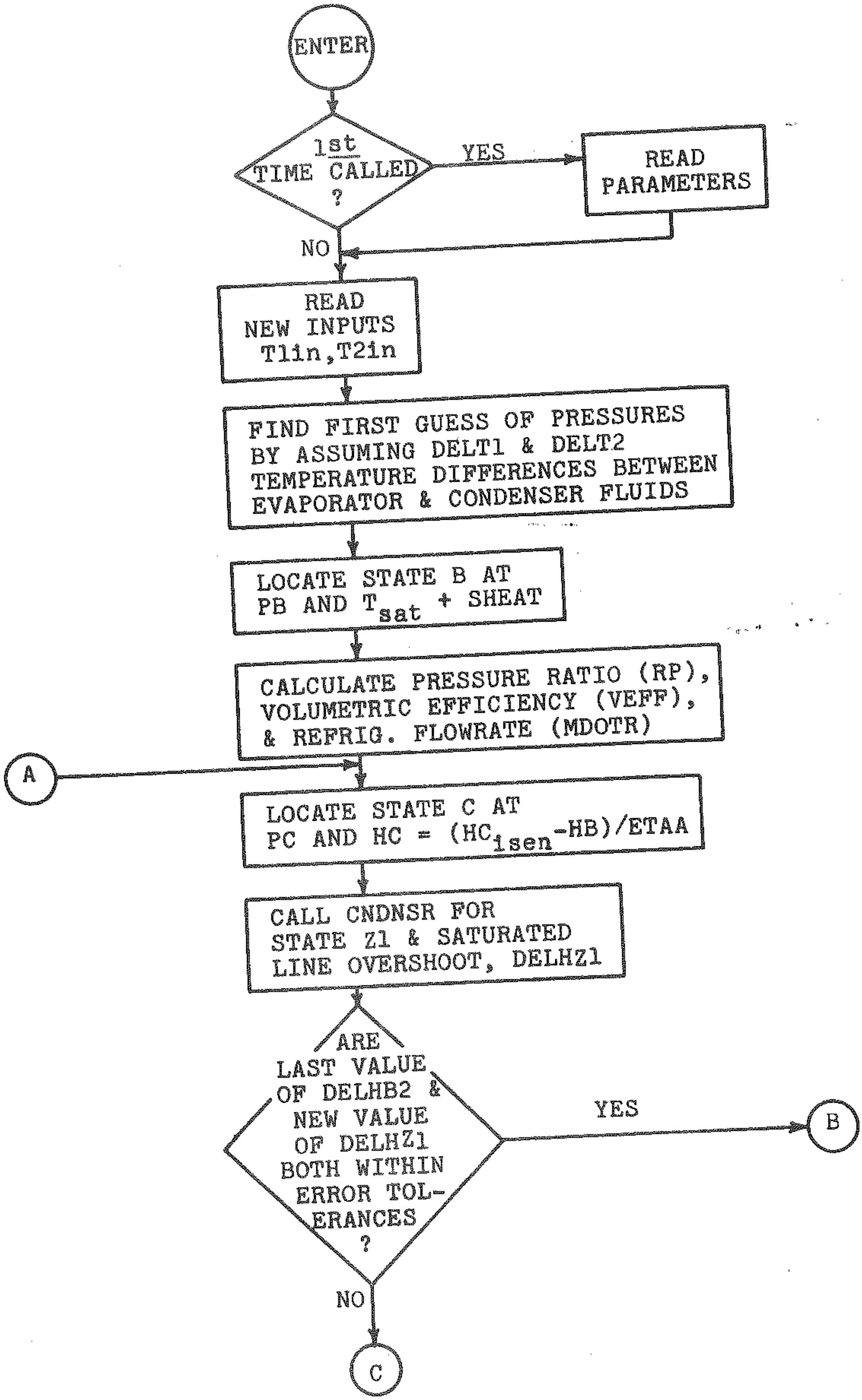

FIG. 2.11 HTPMP LOGIC FLOW DIAGRAM

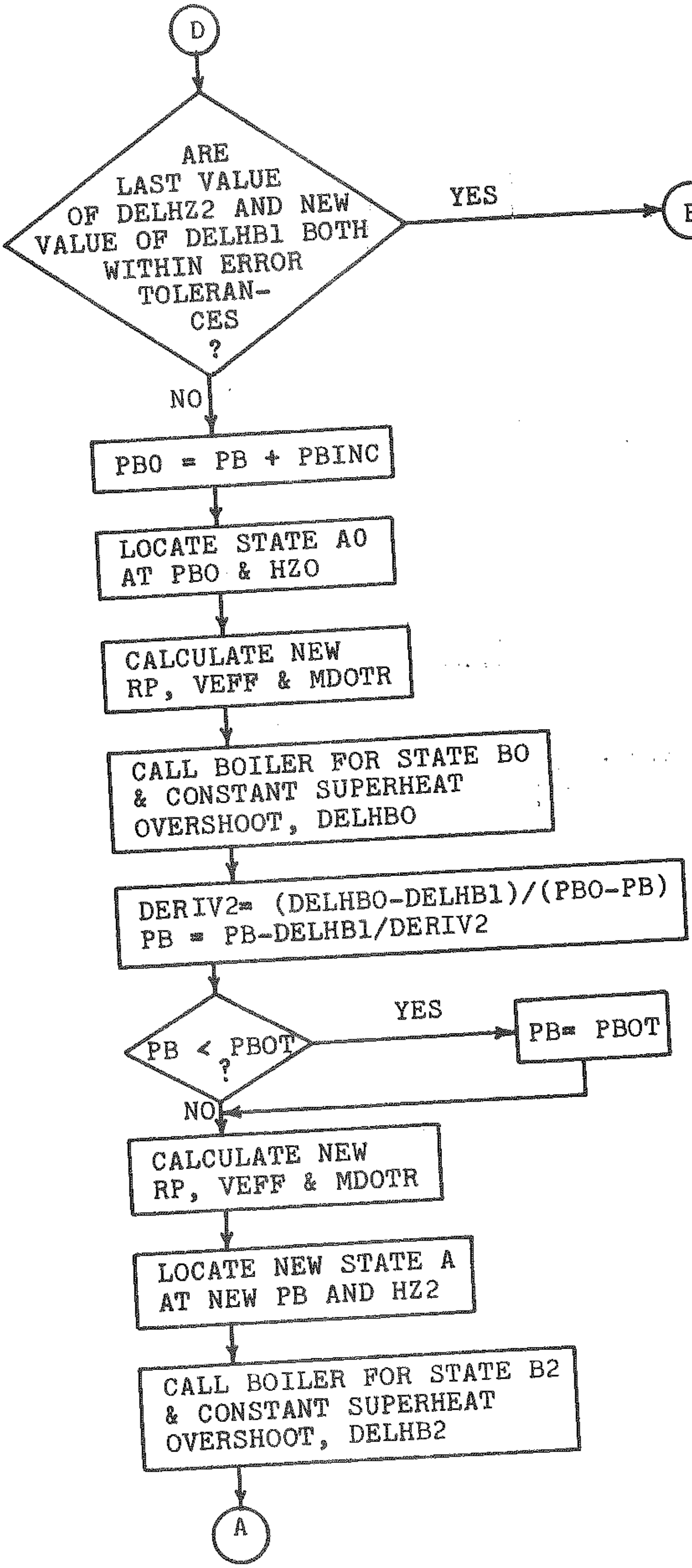

FIG. 2.11 HTPMP LOGIC FLOW DIAGRAM (cont.)

Heat pump capacity would be very high (whenever the evaporator source fluid temperature exceeds the condenser source fluid temperature) were it not for the fact that most heat pumps are not generally designed to operate in this region. As explained in Section 2.3.4, valve and refrigerant charges are simply not large enough to permit increasingly larger capacities as T_{1in} exceeds T_{2in}. Besides this, the HTPMP solution routine becomes increasingly more unstable, and results become increasingly more dependent on the RP_{lim} parameter which, it must be remembered, is an artificial way of enabling the user to specify when refrigerant flow begins to be limited by the expansion valve and/or refrigerant charge (see Section 2.3.4). For these reasons, the pairs T_{1in}, T_{2in} within the cross-hatched area of Fig. 2.12 are not solved for. Instead, QA(I,J) and QR(I,J) for I > J + 1 are assigned values of QA(I,J + 1) and QR(I,J + 1).

The best justification of this procedure, however, is that in a properly designed system the evaporator fluid temperature will never, or hardly ever, exceed the condenser fluid temperature. The heat pump could be provided with an external bypass so that heat may be transferred directly when the "cold" side becomes hotter than the "hot" side. In a simulation, temperatures on both sides can be monitored and steps taken (e.g., larger heat pump and/or heat pump bypass employed) it if is found that T_{1in} frequently exceeds T_{2in}.

When parameter ISAVE is a positive number, DATAPT will save the performance map just created by writing it out on logical unit ISAVE. When ISAVE is a negative number, DATAPT will read the existing performance map off of logical unit -ISAVE. Once a performance map (QA(I,J) and QR(I,J)) exists, the heat pump problem is very quickly and easily solved by subroutine INTERP (listed in Appendix A2.4). When called with an ordered pair T_{1in}, T_{2in}, INTERP finds the 3 X 3 matrixes QA33(L,M) and QR33(L,M) whose center points, L=M=2, represent the closest points to T_{1in} and T_{2in}. Using cubic LaGrangian polynomials, three three-point interpolations are performed to find QA and QR at points 1, 2, and 3 by holding M constant and interpolating in the L direction as shown in Fig. 2.13. Then by holding L constant at T_{1in} and interpolating in the M direction for T_{2in}, QA and QR are both found for T_{1in},T_{2in}. WA is obtained from WA = QR - QA.

2.5 PROGRAM STRUCTURE

Now that all the tasks in the heat pump modeling procedure have been identified and explained, the interrelationships of the routines which perform these tasks can be summed up (see Fig. 2.14). In accordance with the TRNSYS interfacing rules, the "main" program of the heat pump model is a subroutine with a special name (TYPE20). TYPE20 (listed in Appendix A2.1) is a control routine through which TRNSYS (or any main program) interfaces with the actual modeling routines. TYPE20 controls all external input/output operations and the calls to the sizing, operating point solution, performance mapping and interpolation segments of the program. TYPE20 implements the control strategy specified by the user; that is, whether inlet temperatures or heating and cooling demand rates determine when the heat pump will run. TYPE20 ensures that the input exchange fluid temperatures are within their allowable range. It performs unit conversions, if necessary, since a user has the option of working in the standard English system of units or the SI system. If the SI system is employed (as is the case in this work), unit conversion is necessary since the refrigerant property evaluating routine, FREON, and all other internal manipulations are performed in the English system because of greater user familiarity and ease of de-bugging. The TYPE20 logic flowchart is represented in Fig. 2.15.

TYPE20 calls the sizing routine HPSIZE (listed in Appendix A2.2) the first time called in a simulation unless ISAVE is a negative number signifying that a performance map is to be read off of logical unit -ISAVE. HPSIZE locates the design condition states and determines the design condition refrigerant flow rate. It calculates the sizes of individual components as discussed in Section 2.3 and prints out all the sizing information if requested by the user. TYPE20 calls DATAPT, which calls HTPMP repeatedly, to create

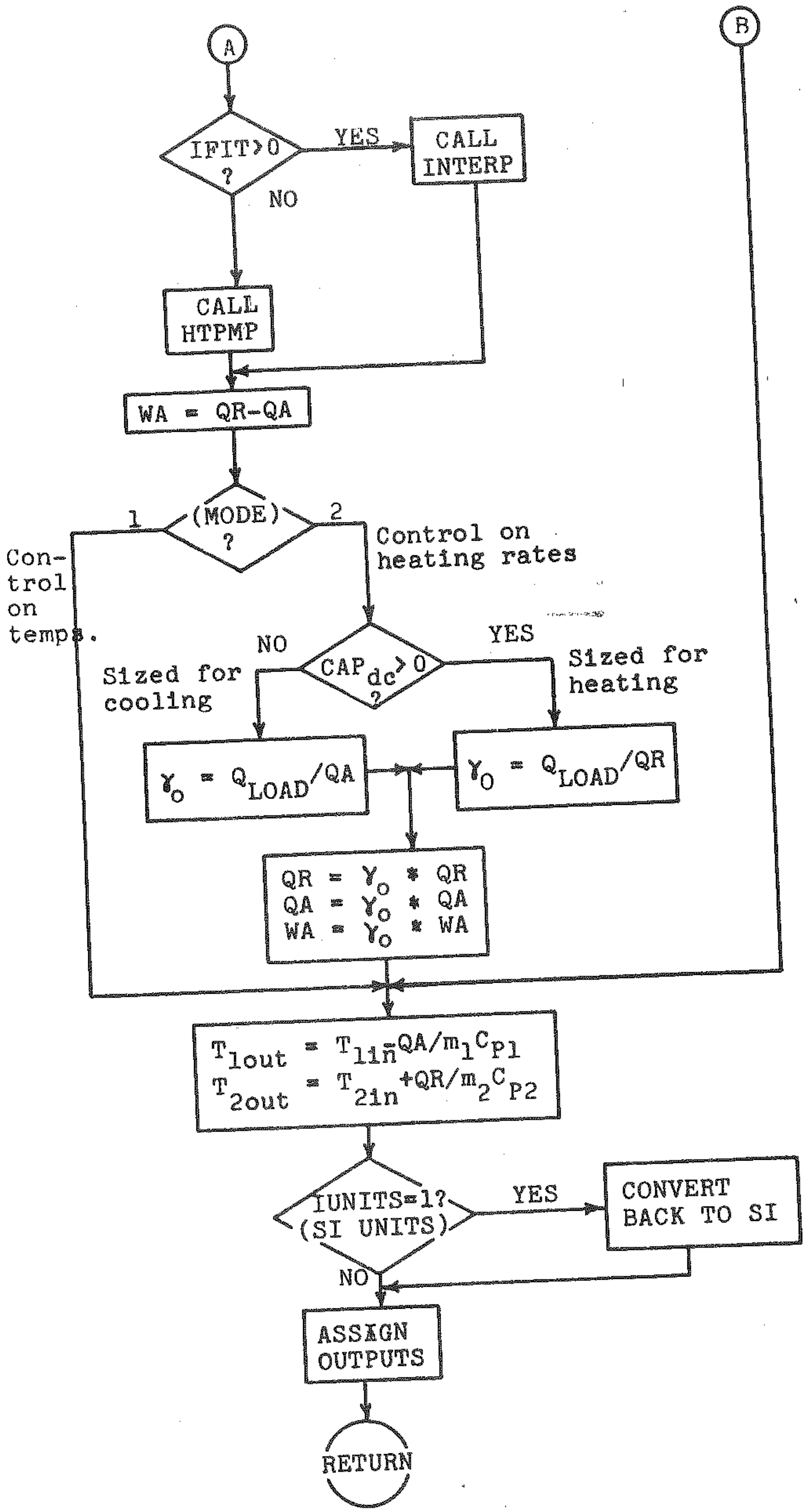

FIG. 2.15 TYPE20 LOGIC FLOWCHART (cont.)

a few different indoor temperatures) are readily available from at least the major manufacturers. Water-to-air heat pumps are produced by a wide variety of small companies (mainly in the southern United States where large bodies of $15^\circ - 25^\circ C$ water are available as both sink and source). Characteristics are available for many of these heat pumps but since they are designed to operate over such a narrow range of temperatures, their characteristics are rather short, straight lines. These are easy enough to duplicate with the model but don't allow verification of operation far from the design point (which is where a heat pump must often operate when solar energy provides the heat source). Finally, water-to-water heat pumps are almost non-existent in the comfort heating and cooling market; ARI lists no manufacturers of unitary water-to-water heat pumps.

Several of the Climate Master water-to-air heat pumps were modeled successfully, if not somewhat inconclusively because of the limited range of the data. Water-to-water performance data was not available, so the main effort in model verification was concerned with air-to-air systems. The three major manufacturers of air-to-air heat pumps used almost exclusively in colder climates are Carrier, G.E. and Westinghouse. The Westinghouse hardware employs a rather unique refrigerant circuit utilizing both suction line and flash tank heat exchangers, and a sub-cool regulating expansion valve, all of which provide for an unusual amount of

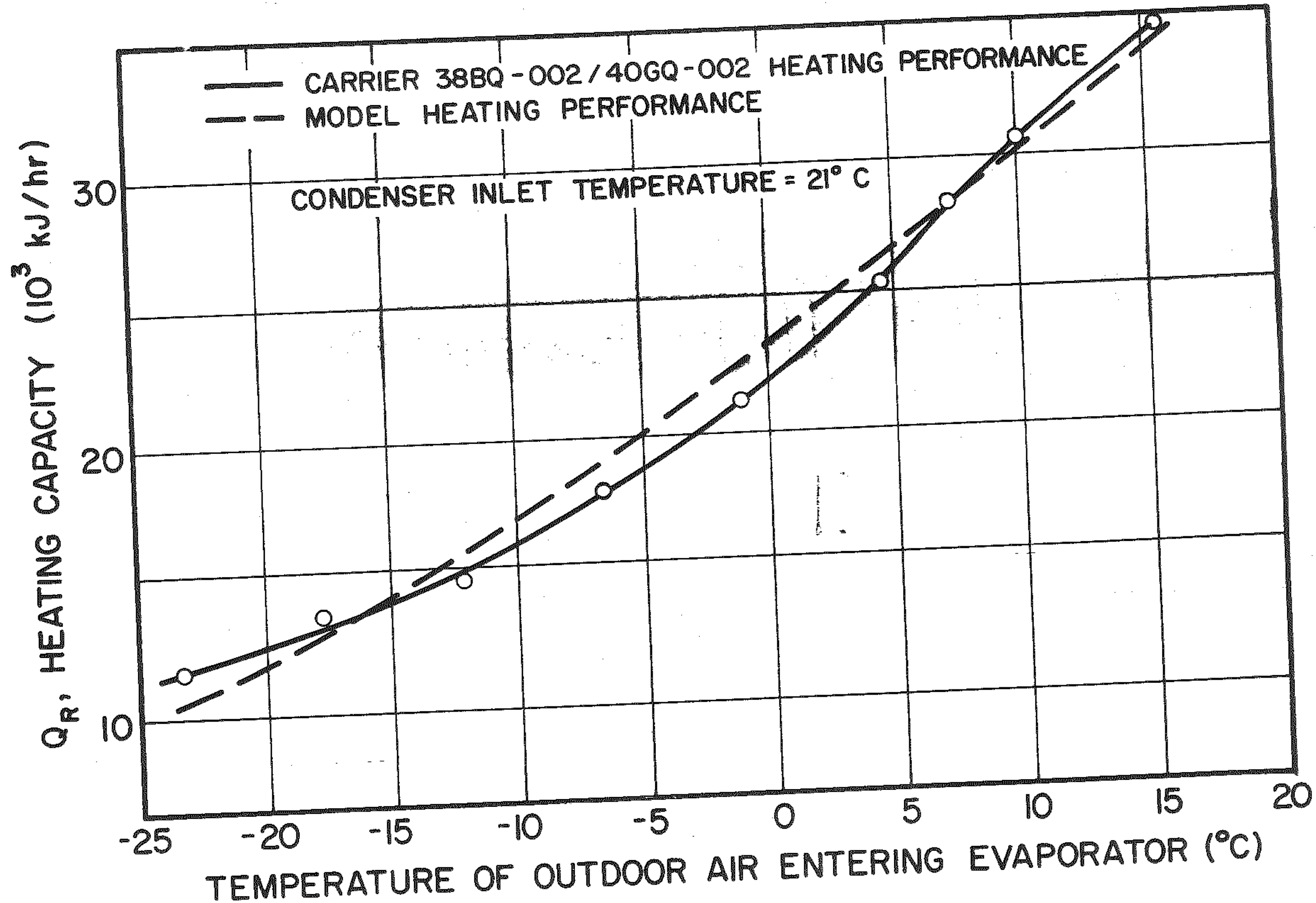

(a) HEATING CAPACITY

COMPARISON OF MODEL TO HARDWARE PERFORMANCE

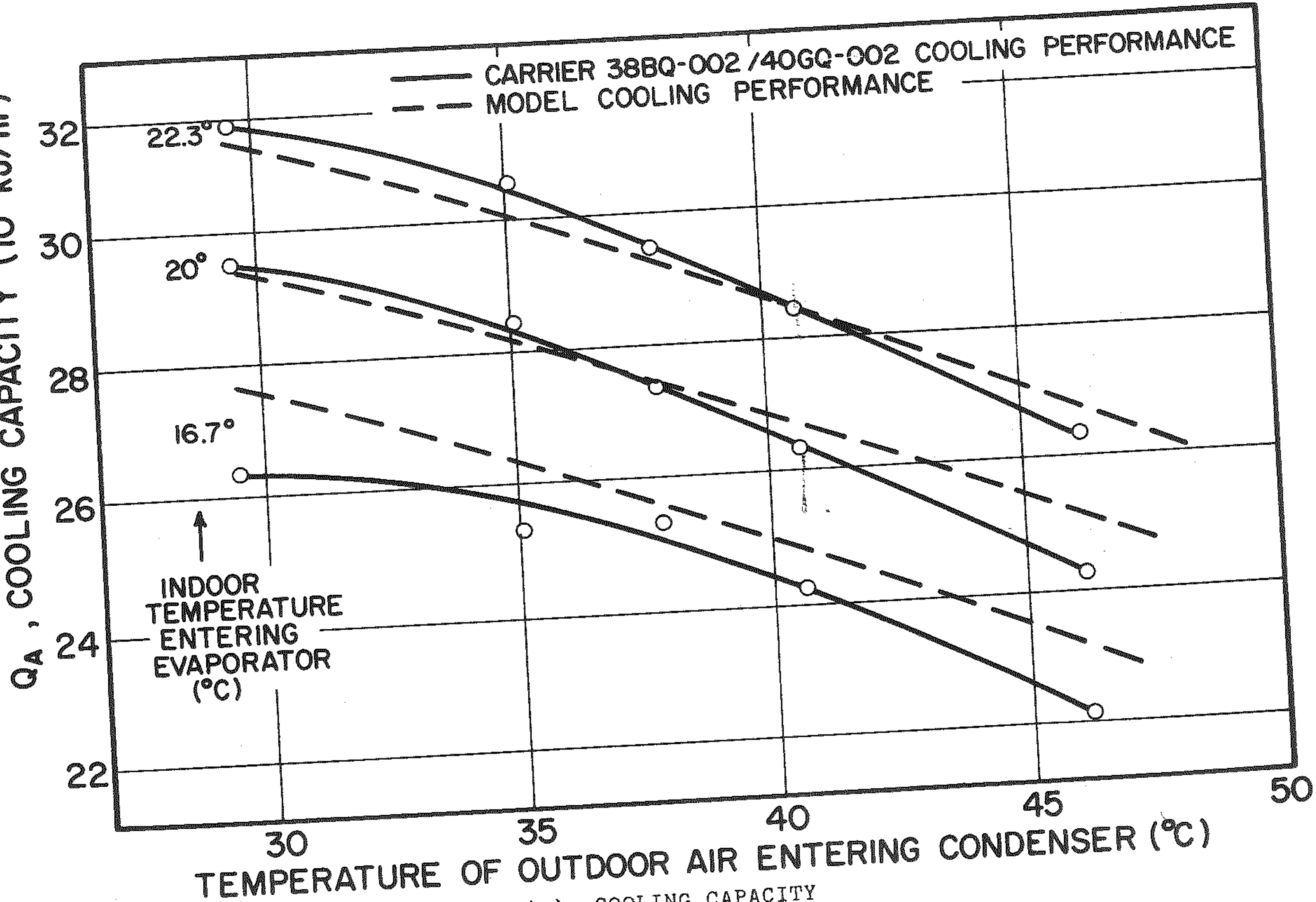

(c) COOLING CAPACITY

... TO HARDWARE PERFORMANCE (cont.)

of different systems in response to identical forcing functions. Actual hourly readings from local weather bureaus of dry bulb temperature, wet bulb temperature, solar radiation intensity, and wind speed provide the raw data used for the simulations. Linear interpolation provides values when needed between hours.

3.1.2 THE COLLECTOR

The Hottel, Whittier, Bliss (4,26,27) flat plate collector model expresses the rate of energy collection, Q_u, as:

$$Q_u = AF_R\left[H_T\tau\alpha - U_L(T_{in} - T_{amb})\right] = \dot{m}C_p(T_o - T_i)$$

where $F_R = \frac{\dot{m}C_p}{AU_L}\left[1 - \exp\left(\frac{F'U_LA}{\dot{m}C_p}\right)\right]$. F', the collector geometry efficiency factor can be determined in the manner given by Bliss (27) or Duffie and Beckman (19). The over-all energy loss coefficient, U_L, is a complicated function of collector construction and operating conditions. It is evaluated from an expression developed by Klein (28).

H_T is the solar energy incident on the tilted surface of the collector and depends on how the measured radiation data available to the program, H, is divided up into beam, H_b, and diffuse, H_d, radiation. H_b and H_d are estimated from an empirical relationship derived from the graphical information of Lui and Jordan (29). Beam radiation incident on the collector is H_bR_b where R_b is a function of the

the indoor-outdoor temperature difference by a significant amount of time, so it can be an important factor in solar system dynamic performance. Another factor is solar heat gain through walls and windows. For these reasons, the simple "degree-hour" TRNSYS load model (where the load is calculated as a constant UA of the house times the outdoor-indoor temperature difference) has been replaced by a more sophisticated load model with subroutines that treat heat transfer through each wall, the roof and the basement separately. The walls are treated as three planer nodes each having a mass and specific heat commensurate with the wall construction. An energy balance is performed for each node, and the resulting set of algebraic and differential equations are solved for the heat transferred into or out of the room. The same routine which finds R_b, the ratio of incident solar energy on a collector surface of known orientation to that on a horizontal surface, is used to calculate the instantaneous radiation on each of the walls and the roof. Percent windows and percent shading are accounted for, as is infiltration and internal heat generation.

3.2 SYSTEMS DESCRIPTION

On the basis of previous work (1-6) and to limit the scope of this study, two "standard" system designs were chosen for detailed performance study. These systems are by no means equivalent to the full range of possible solar

		PARALLEL HEAT PUMP SYSTEM (I)		IN-LINE HEAT PUMP SYSTEM (II)	
		1.5 ton (A)	3.0 ton (B)	1.5 ton (A)	3.0 ton (B)
COLLECTOR AREA	0 m^2	IA00	IB00	—	—
	10 m^2	IA10	IB10	—	—
	20 m^2	IA20	IB20	IIA20	IIB20
	30 m^2	IA30	IB30	IIA30	IIB30
	40 m^2	IA40	IB40	IIA40	IIB40

TABLE 3.1 RUN SUMMARY

	PARAMETER	VALUE
AIR-TO-AIR HEAT PUMPS	Capacity (at 20°C indoor/-6.7°C outdoor (Runs IAXX)	18990 kJ/hr (1.5 tons)
	(Runs IBXX)	37980 kJ/hr (3.0 tons)
	Indoor Coil Air Flowrate (Runs IAXX)	2045 kg/hr
	(Runs IBXX)	4091 kg/hr
	Outdoor Coil Air Flowrate (Runs IAXX)	4091 kg/hr
	(Runs IBXX)	8182 kg/hr
	Minimum Evaporator Inlet Temperature	-25°C
	Maximum Condenser Inlet Temperature	40°C
	Adiabatic Compression Efficiency, η_a	0.7
	Refrigerant	R-22
	Design Evaporator Outlet Temperature Difference	3°C
	Design Condenser Outlet Temperature Difference	6°C
	Design Boiling Heat Transfer Coefficient	16350 kJ/m^2-hr-°C
	Design Condensing Heat Transfer Coefficient	6133 kJ/m^2-hr-°C
	Design Superheated Vapor Heat Transfer Coeff.	1635 kJ/m^2-hr-°C
	Evaporator Air Side Heat Transfer Coeff.	2044 kJ/m^2-hr-°C
	Condenser Air Side Heat Transfer Coeff.	1227 kJ/m^2-hr-°C
	Evaporator Air to Refrigerant Area Ratio	5
	Condenser Air to Refrigerant Area Ratio	10
	Evaporator Outlet Superheating	7°C
	Condenser Outlet Subcooling	0°C
	Pressure Ratio at Which Valve is Wide Open	2
	Fraction Capacity Lost below Freezing Due to Evaporator Coil Frost & Defrost	0.05
WATER-TO-WATER HEAT PUMPS	Capacity (at 20°C evap.inlet/60°C cond. inlet) (Runs IIAXX)	18990 kJ/hr (1.5 tons)
	(Runs IIBXX)	37980 kJ/hr (3.0 tons)
	Water Flow Rate (Runs IIAXX)	820 kg/hr
	(Runs IIBXX)	1640 kg/hr
	Minimum Evaporator Inlet Temperature	0°C
	Maximum Condenser Inlet Temperature	80°C
	Adiabatic Compression Efficiency, η_a	0.6
	Refrigerant	R-114
	Design Evaporator Outlet Temperature Difference	4°C
	Design Condenser Outlet Temperature Difference	5°C
	Design Boiling Heat Transfer Coefficient	16350 kJ/m^2-hr-°C
	Design Condensing Heat Transfer Coeff.	6133 kJ/m^2-hr-°C
	Design Superheated Vapor Heat Transfer Coeff.	1635 kJ/m^2-hr-°C
	Evaporator Water Side Heat Transfer Coeff.	2452 kJ/m^2-hr-°C
	Condenser Water Side Heat Transfer Coeff.	2452 kJ/m^2-hr-°C
	Evaporator Water to Refrigerant Area Ratio	4
	Condenser Water to Refrigerant Area Ratio	4
	Evaporator Outlet Superheating	7°C
	Condenser Outlet Subcooling	0°C
	Pressure Ratio at Which Valve is Wide Open	2

TABLE 3.2 COMPONENT PARAMETERS (cont.)

All systems studied here are simulated using the same year of meteorological data and the same heating and cooling load models. The weather data is from the Albuquerque weather bureau for 1959. This location was selected on the basis of previous feasibility studies (1-6) and availability of data.

The space heating and cooling load parameters represent the Colorado State University Solar House I (18). The house is a single story wood frame structure having 140 m^2 of floor area. It has a basement and a vented attic. The house's over-all design loss coefficient is approximately 1250 kj/^oC-hr. The loads differ slightly with collector area since tank losses are counted as heat inputs to the conditioned space. The load model has been calculated with consideration of capacitance, solar heat gains through walls, roof and windows, infiltration, and internal generation. The load model parameters are listed in Table 3.2.

3.2.1 THE PARALLEL SYSTEM

The "parallel" system collector has a non-selective surface and two covers of medium quality glass. In the heating mode (Fig. 3.1a), the load controller switches the pumps on and off to extract enough energy from the tank to meet the load. If the load cannot be met, the controller also switches on the parallel air-to-air heat pump to meet the balance. If that is still insufficient to meet the load, the heat pump's built-in auxiliary heater (electrical resistance heaters) make up the rest.

In the cooling mode (Fig. 3.1b), the solar collection system needs only to meet the service hot water load (which it can do very easily). The load controller switches the heat pump on and off to meet the cooling load. There is no cooling auxiliary so shortages of heat pump cooling capacity represent times when the indoor temperature would rise above the room design temperature.

The heat pumps used in the "parallel" mode are designed to yield 1.5 and 3.0 tons (18991 kJ/hr and 37982 kJ/hr) at design condition evaporator and condenser air inlet temperatures of -6.7°C and 20°C. They employ cross flow heat exchangers and refrigerant R-22. Other important parameters used to model these devices are listed in Table 3.2. These air-to-air heat pumps are modeled to very closely represent the performance of the Carrier unit described in Section 2.6. (It should be noted that the heat pumps modeled here supply their "rated" capacities at a lower outdoor temperature than is normally used in the industry. These heat pumps are essentially "de-rated" approximately 50 to 60% in comparison to industry standards.)

3.2.2 IN-LINE SYSTEM

Fig. 3.2a shows the in-line solar energy-heat pump system with evaporator side storage in the heating mode.

The collector used here has a single glass cover since it will be operating at lower temperatures. Though the service hot water system is identical to the parallel system, the tank temperature will be lower so less of the service hot water load can be met by solar during mid-winter.

The in-line heat pumps are designed to supply 1.5 tons and 3.0 tons of heating capacity at design condition evaporator and condenser water inlet temperatures of 20°C and 60°C. They utilize parallel-counterflow water to refrigerant evaporators and condensers, and refrigerant R-114. Important parameters used in the model are listed in Table 3.2.

In the heating mode there are two submodes for transferring tank energy to the load depending on tank temperature. If the temperature exceeds 30°C, the bypass controller positions the diverter valves to deliver hot water directly to the load heat exchanger, bypassing the heat pump. When the tank temperature dips below 30°C, the diverter valves are re-positioned to deliver the tank outlet to the heat pump evaporator side and the load outlet to the heat pump condenser side. The heat pump is simultaneously switched on. The heat pump has its own internal control criteria that will turn itself off to prevent freeze-up of the evaporator as the tank temperature approaches 0°C. In either heating submode, if the load heat exchanger cannot extract enough energy from the inlet flowstream to meet the load, the balance is made up by a "parallel" auxiliary which is assumed to be some kind of "conventional" heat source.

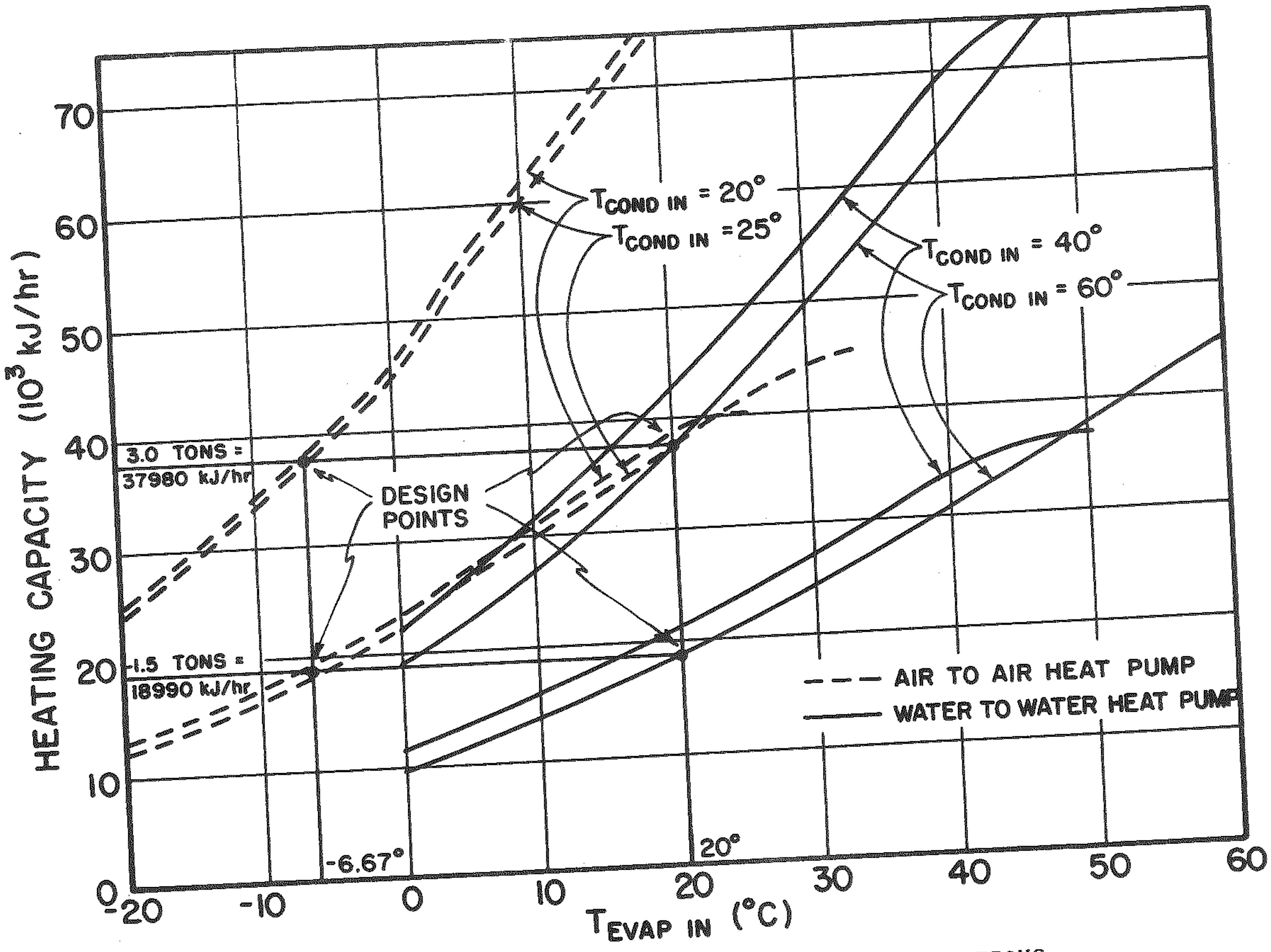

FIG. 3.3a PERFORMANCE OF HEAT PUMPS USED IN SIMULATIONS

The "total auxiliary" requirement referred to above is the difference between the total load and the energy supplied by the solar system. The "actual auxiliary" energy required by these systems consists of heat pump compressor and fan motor electrical input (W_{HP}), heat pump auxiliary heat (Q_{HPAUX}), and service hot water auxiliary (Q_{SHWA}) (neglecting the small water pumping power). It is reasonable to assume that for practical systems, the latter two energy requirements would also be met with electricity. An average system COP can then be defined for the heating season as the "total auxiliary" energy requirement divided by the total electrical energy input. This system COP is a function of collector area and heat pump size as shown in Fig. 3.5.

The cooling mode performance is a function of heat pump size, but not collector area. The 1.5 ton heat pump meets 99% of the cooling load and the 3 ton heat pump meets 100% of the load. The larger heat pump requires slightly less electrical input.

The results of the in-line system simulations are shown by months in Table 3.4. The fraction of the total load met by solar energy, F_s, is defined in the same manner as in the parallel system. The in-line heat pump electrical requirements (W_{HP}) are considered to be auxiliary. Here, however, F_s is a function of both collector area and heat pump size as shown in Fig. 3.6. Comparison of Fig. 3.4 and Fig. 3.6 reveals that all F_s curves are very nearly identical. The

1.5 TON IN-LINE HEAT PUMP

	COLLECTOR AREA (m^2)	SPACE HEATING OR COOLING LOAD Q_L (10^6kJ)	NET SOLAR ENERGY GAIN (Q_u-Q_{DUMP}) Q_{SG}(10^6kJ)			SERVICE HOT WATER AUXILIARY REQUIRED Q_{SHWA} (10^6kJ)			HEAT PUMP ELECTRICAL INPUT W_{HP} (10^6kJ)			SPACE HEATING AUXILIARY REQUIRED Q_{AUX} (10^6kJ)			FRACTION OF LOAD MET BY SOLAR F_s		
		0	20	30	40	20	30	40	20	30	40	20	30	40	20	30	40
HEATING SEASON	Oct	3.53	4.88	5.48	5.89	0.24	0.14	0.06	0.24	0.03	0.00	0.01	0.00	0.00	0.90	0.96	0.99
	Nov	7.52	7.18	8.70	9.35	0.91	0.55	0.26	1.09	0.31	0.03	0.60	0.12	0.00	0.85	0.89	0.97
	Dec	10.22	5.80	7.84	9.26	1.22	1.06	0.91	1.55	1.37	1.21	3.66	1.88	0.58	0.46	0.69	0.77
	Jan	11.21	7.68	10.23	11.83	1.12	0.92	0.69	1.97	1.33	0.53	2.77	1.20	0.77	0.54	0.73	0.84
	Feb	9.46	7.09	8.96	10.17	1.04	0.80	0.59	1.43	0.75	0.39	2.11	1.13	0.47	0.59	0.76	0.87
	Mar	7.25	7.76	8.84	9.22	0.67	0.30	0.09	0.63	0.08	0.00	0.26	0.05	0.00	0.82	0.95	0.99
	Apr	4.45	5.91	6.60	6.94	0.43	0.15	0.03	0.25	0.00	0.00	0.01	0.00	0.00	0.88	0.97	1.00
	TOTAL	53.64	46.30	56.65	62.66	5.63	3.92	2.63	7.16	3.87	2.16	9.42	4.38	1.82	0.66	0.81	0.89
COOLING SEASON	Apr	3.13		N/A			0.00			0.86			0.12 *			N/A	
	May	3.95					0.00			1.15			0.08				
	Jun	7.46					0.00			2.28			0.72				
	Jul	7.83					0.00			2.38			0.86				
	Aug	7.25					0.00			2.14			0.99				
	Sep	8.60					0.00			2.10			2.09				
	TOTAL	38.22					0.00			10.91			4.86				

3.0 TON IN-LINE HEAT PUMP

	COLLECTOR AREA (m^2)	NET SOLAR ENERGY GAIN (Q_u-Q_{DUMP}) Q_{SG}(10^6kJ)			SERVICE HOT WATER AUXILIARY REQUIRED Q_{SHWA}(10^6kJ)			HEAT PUMP ELECTRICAL INPUT W_{HP}(10^6kJ)			SPACE HEATING AUXILIARY REQUIRED Q_{AUX}(10^6kJ)			FRACTION OF LOAD MET BY SOLAR F_s		
		20	30	40	20	30	40	20	30	40	20	30	40	20	30	40
HEATING SEASON	Oct	4.59	5.21	5.62	0.24	0.13	0.05	0.18	0.01	0.00	0.04	0.00	0.00	0.91	0.97	0.99
	Nov	7.33	8.60	8.81	0.93	0.52	0.20	0.93	0.25	0.00	0.51	0.00	0.00	0.74	0.91	0.98
	Dec	5.86	7.96	9.15	1.24	1.09	0.89	1.23	1.21	0.96	3.87	1.84	0.76	0.47	0.65	0.77
	Jan	7.73	10.68	12.22	1.12	0.98	0.73	1.68	1.63	0.83	2.95	1.80	0.01	0.55	0.73	0.88
	Feb	7.25	9.14	10.07	1.08	0.83	0.57	1.18	0.73	0.34	2.13	0.57	0.40	0.60	0.81	0.88
	Mar	7.83	8.67	8.55	0.67	0.27	0.06	0.55	0.08	0.00	0.25	0.00	0.00	0.91	0.96	0.99
	Apr	5.74	6.20	6.39	0.40	0.11	0.01	0.23	0.00	0.00	0.00	0.00	0.00	0.89	0.98	1.00
	TOTAL	46.33	56.46	60.81	5.68	3.93	2.51	5.98	3.91	2.13	9.75	3.21	1.17	0.67	0.83	0.91
COOLING SEASON	Apr		N/A			0.00			0.57 *			0.01			N/A	
	May					0.00			0.68			0.02				
	Jun					0.00			1.70			0.02				
	Jul					0.00			1.87			0.01				
	Aug					0.00			3.02			0.03				
	Sep					0.00			2.02			0.25				
	TOTAL					0.00			9.86			0.34				

* In the cooling season, Q_{AUX} represents the cooling load not met

TABLE 3.4 IN-LINE SYSTEM SIMULATION RESULTS conclusion is that the collector efficiency gained by operating at a lower tank temperature has been offset (in these examples) by increased losses associated with the one cover collector. Approximately the same amount of auxiliary heat (Q_{AUX}) must be added to the in-line system as was required by the "parallel" system. Now, however, instead of an air-to-air heat pump providing this function, a conventional heat source must be used. Clearly, no matter what kind of auxiliary is used, the cost of meeting this substantial load is going to be significant. A fuel burning furnace would cost less to run than resistance heaters but would be an additional initial equipment cost. Assuming the in-line system utilizes electricity for service hot water auxiliary and heat pump compressor work only (again neglecting pump work), Fig. 3.7 has been drawn to show the minimum fraction of auxiliary energy that must be electric, F_E, as a function of collector area and heat pump size.

In the cooling mode, the in-line system 1.5 and 3 ton heat pumps provide 87% and 99% of the cooling load but use slightly less electric power than the air-to-air heat pumps. The 3 ton heat pump again uses less energy even though it meets much more of the load.

A factor which further tends to even out the differences between the parallel and in-line system performance is the hot water load. The main storage tank in the parallel system is maintained at a much higher average temperature than the in-line system's storage tank. As a result, more of the service hot water load can be transferred across the heat exchanger between the main storage tank and the service hot water pre-heat tank during the heating season as evident from Figs. 3.4 and 3.5. Thus, less service hot water auxiliary is required for the parallel heat pump system.

3.4 AN ECONOMIC EVALUATION

A complete economic analysis is beyond the scope of this study. It would require plotting of annual costs vs collector area and heat pump size assuming different combinations of equipment, electricity, and fuel costs. The thermal performance has been computed without regard to costs and provides a basis for an economic analysis as in the example presented below. The thermal performance results have been presented in a way that enables easy re-evaluation of the economics using different cost assumptions. However, the thermal performance simulations are limited in their scope, and caution should be exercised in drawing general conclusions from them.

The annual "cost above base" is computed for each system by summing the annual amortized equipment "cost above base" and the annual electrical and fuel costs. Annual fixed costs are assumed to be 12% of the investment. The base system is defined as a 1.5 ton air-to-air heat pump (which is just large enough to meet the cooling load) with built-in

		Cost/Unit	PARALLEL SYSTEMS										IN-LINE SYSTEMS					
			1.5 TON HEAT PUMP					3.0 TON HEAT PUMP					1.5 TON HEAT PUMP			3.0 TON HEAT PUMP		
			IA00	IA10	IA20	IA30	IA40	IB00	IB10	IB20	IB30	IB40	IIA 20	IIA 30	IIA 40	IIB 20	IIB 30	IIB 40
EQUIPMENT	1 Cover Collector	$\$50/m^2$											1000	1500	2000	1000	1500	2000
	2 Cover Collector	$\$70/m^2$	0	700	1400	2100	2800	0	700	1400	2100	2800						
	Collector Pumps, Valves, Controller & Heat Exchanger	-	200	200	300	400	500	200	200	300	400	500	300	400	500	300	400	500
	Storage Tank[1]	-	300	400	500	600	700	300	400	500	600	700	500	600	700	500	600	700
	Heat Pump, Valves, Controller	-	0	0	0	0	0	1000	1000	1000	1000	1000	0	0	0	1000	1000	1000
	Cooling Tower	-											400	400	400	400	400	400
	TOTAL (C_{EQPMT})		500	1300	2200	3100	4000	1500	2300	3200	4100	5000	2200	2900	3600	3200	3900	4600
ENERGY	Hot Water Auxil	$\$11.11/10^6kJ$	211	65	49	31	17	211	65	49	31	17	63	44	29	63	44	28
	Heat Pump Elect. (winter)	"	199	133	68	28	11	194	133	71	29	10	80	43	24	66	43	24
	(summer)	"	136	136	136	136	136	127	127	127	127	127	121	121	121	110	110	110
	Space Heating Auxil (winter only)	"	37	35	23	11	3	3	1	1	0	0	105	49	20	108	36	13
	TOTAL (C_{ENERGY})		583	369	276	206	167	535	326	248	187	154	369	257	194	347	233	175
	C.A.B.=(C_{EQPMT}).12+C_{ENERGY}		643	525	540	578	647	715	602	632	679	754	633	605	626	731	701	727

[1]Storage tank costs from GE-Phase 0 Report

TABLE 3.5 COSTS ABOVE BASE

system heat pumps, unlike the parallel heat pumps, rely on collected solar energy as a source in the heating mode. The smaller collectors simply cannot furnish an adequate heat source in the in-line configuration. It is also apparent from Fig. 3.8 that the improved performance of the 3 ton heat pump in either configuration does not compensate for its higher first cost.

3.5 CONCLUSIONS AND RECOMMENDATIONS

A general method of modeling single stage heat pumps has been described. "Typical" performance maps have been constructed for air-to-air and water-to-water heat pumps. Two solar energy-heat pump systems have been described and simulated using the transient simulation capabilities of TRNSYS. The resultant thermal performance data revealed some very interesting information about the two basic design philosophies considered here. It is recognized that neither of these systems has been optimized insofar as most system parameters are concerned. No one has yet ascertained what design constraints should apply to system parameters, or indeed, what the most important parameters actually are. Nonetheless, the same basic trends noted in these study cases are bound to apply in more carefully optimized systems of the same design.

First of all, higher collector efficiencies <u>can</u> be expected from in-line systems since the collectors operate always capable of meeting the auxiliary requirement with a COP of greater than unity.

An "improved" solar-heat pump system can be envisioned that could incorporate the advantages of both the in-line and the parallel systems. The heat pump could use storage as the heat source when the storage temperature is sufficiently high. When storage is depleted, the heat pump could switch to outdoor air as a source. For water collector systems, the heat pump would probably have to have both an air source and a water source evaporator for the heating mode. This is an additional complexity to the system but may actually not require a net first cost increase since the cooling tower formerly used for summer heat rejection could be replaced by the air source outdoor coil used as both a winter heat source and a summer heat sink.

The example economic analysis reveals that the parallel solar energy heat pump system is slightly less costly than a heat pump system working alone. The economic incentive for using the former would increase for lower solar equipment cost or higher electric costs. The economic attractiveness of a combination in-line/parallel system is almost a surety based on these findings.

The effects of climate are unclear. It is not obvious that the same considerations that make solar systems or heat pump systems more or less feasible in certain climates apply to solar-heat pump systems in general. The attractiveness

APPENDIX

G, and the air properties. Air property changes have very little effect on h over a wide range of temperatures. The increase of k and μ with temperature is offset by the decrease in ρ (which is proportional to G). Evaluated at $50^{o}F$, equation A1.2 becomes $h_{air} = .049\ 10^{B} r_{h}^{-.4} G^{.6}$. This relationship provides a convenient air side heat transfer correlation for a wide variety of different surfaces whose "B" values can be easily inserted.

These equations can be simplified by removing groups of constants. All U's, T's and Q's are known at design conditions.

THEN:

1. $\varepsilon_{2P} = 1 - e^{-NTU_{2P}}$
2. $\varepsilon_{2P} = \beta A_{RT}/A_{R2P}$
3. $NTU_{2P} = \alpha A_{RT}$
4. $\varepsilon_{SH} = \sigma(A_{RT}/A_{RSH})(1 - \exp\left[-(1 - e^{-NTU_{SH}})((A_{RSH}/A_{RT})/\sigma)\right])$
5. $\varepsilon_{SH} = \tau(A_{RT}/A_{RSH})$
6. $NTU_{SH} = \delta A_{RT}$
7. $A_{RT} = A_{RSH} + A_{R2P}$

WHERE:

1. $\alpha = U_{2P}/CC2$
2. $\beta = QR_{2P}/CC2(TY-T2INDC)$
3. $\delta = U_{SH}/CC2$
4. $\sigma = CC_{RSH}/CC2$
5. $\tau = QR_{SH}/CC2(TC-T2INDC)$
6. $\theta = -\sigma \ln(1 - \tau/\sigma)$
7. $\phi = 1 - \theta - \beta$

This system reduces to:

$$(1-\beta)e^{-\delta A_{RT}} + (1-\theta)e^{-\alpha A_{RT}} - e^{-(\alpha+\delta)A_{RT}} - \phi = 0$$

which is solved with Newton's method for A_{RT} in subroutine HPSIZE.

The endstates of the condenser process are calculated in subroutine CNDNSR once A_{RT} has been determined by the sizing routine. First, the amount of heat exchanger area used to de-superheat the vapor, A_{RSH}, is found by solving A1.2-1, 2 & 3 below. (The heat rejected in the superheat exchanger, QR_{SH} is known from the inlet refrigerant mass flowrate and the states C and Y are known from Fig. 2.1.) The endstates are the same for either fluid having maximum capacitance. For C_{min} = capacitance of superheated refrigerant = CC_{RSH}, the equations are:

A1.3 WATER SOURCE CONDENSER EQUATIONS

As discussed in Section 2.3.2.2, an exact solution for almost any water-source condenser flow configuration other than simple parallel flow is very difficult. It is assumed in this analysis that the two heat exchangers (superheat and 2-phase) can be separated and solved independently. Both of these heat exchangers are represented by the parallel-counterflow ε-N_{tu} equations (though, as pointed out previously, these equations reduce to the same simple form for any flow arrangement in the 2-phase heat exchanger). The water temperature entering the superheat exchanger is T2IN, the condenser water inlet temperature. The water temperature entering the 2-phase exchanger is T22P = T2IN - QR_{SH}/CC2 where QR_{SH} is the heat exchanged in the superheat exchanger and CC2 = $\dot{m}_2 C_{p2}$ is the total water side capacitance. This assumes that <u>all</u> the water entering the condenser first flows through the superheat exchanger, then through the 2-phase exchanger.

In the sizing routine, QR_{SH}, QR_{2P}, TC, TY and T22P are known at design conditions. Design condition effectivenesses can then be found from $\varepsilon = QR/C_{min}(\Delta T_{max})$. The parallel-counterflow heat exchanger equations can then be solved for UA_{dc}'s in both heat exchangers at design conditions.

Thus, $\varepsilon_{2P} = 1 - e^{-U_{R2P}A_{R2P}/CC2}$ (A1.3-6)

and, $QR_{2P} = CC2\ \varepsilon_{2P}\ (T22P-TY)$ (A1.3-7)

where T22P is the temperature of the water after passing through the superheat exchanger:

$$T22P = T2IN - QR_{SH}/CC2$$

then, $T2OUT = T2IN - (QR_{SH}+QR_{2P})/(\dot{m}C_p)_{water}$ (A1.3-8)

```
      ETAA=PAR(10)
      PMAX=PAR(11)
      IFIT=PAR(12)
      ISAVE=PAR(13)
      HBOILO=PAR(14)
      H1=PAR(15)
      ICHX=PAR(16)
      SHEAT=PAR(17)
      DELT1=PAR(18)
      DELT2=PAR(19)
      IUNITS=PAR(20)
      IPRSZ=PAR(21)
      RPII=PAR(22)
      CFROST=PAR(23)
      HR2P=PAR(24)
      HRSHD=PAR(25)
      H2=PAR(26)
      AREVAP=PAR(27)
      ARCOND=PAR(28)
      IPP=PAR(29)
      MODE=PAR(30)
      IF(ISAVE.GE.0)  CALL HPSIZE(PAR)
      IF(IFIT) 20,20,15
15    CALL DATAPT(PAR)
20    DO 21 I=1,6
21    XIN(I)=X(I)
      GO TO (22,23),IUNITS
22    CONTINUE
C  CONVERT SI TO ENGLISH
      XIN(1)=X(1)*1.8+32.
      XIN(2)=X(2)/.45359
      XIN(3)=X(3)*1.8+32.
      XIN(4)=X(4)/.45359
      XIN(6)=X(6)/1.05506
23    CONTINUE
      T1IN=XIN(1)
      M1DOT=XIN(2)
      T2IN=XIN(3)
      M2DOT=XIN(4)
      IGAM=XIN(5)
      QLOAD=XIN(6)
      IF(IGAM.LE.0) GO TO 600
      IF(T1IN.LE.T1MIN) GO TO 600
      IF(T2IN.GE.T2MAX) GO TO 600
      IF(IFIT) 30,30,25
25    CALL INTERP(T1IN,T2IN,QA,QR)
      GO TO 500
30    CALL HTPMP(PAR,XIN,QA,QR)
500   WA=QR-QA
      ON=0.0
      IF(WA.LE.0.0)  GO TO 600
      ON=1.0
510   GO TO (540,520),MODE
520   CONTINUE
C  HEAT PUMP CONTROLLED ON HEATING RATES
      IF(QR.LE.1.0.OR.QLOAD.LE.0.0) GO TO 600
      IF(PAR(1)) 524,522,522
```

```
      DATA CPLIQP/.335/
C  VARIABLES SUFFIXED WITH 1 REFER TO EVAPORATOR SIDE
C  VARIABLES SUFFIXED WITH 2 REFER TO CONDENSER SIDE
      CAPDC=PAR(1)
      CP1=PAR(2)
      CP2=PAR(3)
      T1INDC=PAR(4)
      M1DOTD=PAR(5)
      T2INDC=PAR(6)
      M2DOTD=PAR(7)
      T1MIN=PAR(8)
      T2MAX=PAR(9)
      ETAA=PAR(10)
      PMAX=PAR(11)
      IFIT=PAR(12)
      ISAVE=PAR(13)
      HPOILD=PAR(14)
      H1=PAR(15)
      ICHX=PAR(16)
      SHEAT=PAR(17)
      DELT1=PAR(18)
      DELT2=PAR(19)
      IPRSZ=PAR(21)
      RPII=PAR(22)
      CFROST=PAR(23)
      HR2P=PAR(24)
      HRSHD=PAR(25)
      H2=PAR(26)
      AREVAP=PAR(27)
      ARCOND=PAR(28)
      CAPDCC=CAPDC
      IF(CFROST.GT.0.0.AND.T1INDC.LT.40.) CAPDCC=CAPDC/(1.-CFROST)
C  DETERMINATION OF STATES AT DESIGN CONDITIONS
C  CAPDC IS POSITIVE FOR HEATING, NEGATIVE FOR COOLING
      IF(CAPDC)  35,30,30
C  HEATING MODE (ASSUME COP=5 AT D.C. TO GET APPROX QADC=0.8*CAPDC)
30    IMODE=1
      QRDC=CAPDCC
      QADC=0.8*CAPDCC
      GO TO 40
C  COOLING MODE (ASSUME COP=4 AT D.C. TO GET APPROX QRDC=-1.25*CAPDC)
35    IMODE=2
      QADC=-CAPDCC
      QRDC=-1.25*CAPDCC
C  T2 IS DELT2 DEGREES GREATER THAN OUTLET CONDENSER FLUID TEMP.
40    T2OUTD=T2INDC+QRDC/(CP2*(M2DOTD*M2DOT))
      T2=T2OUTD+DELT2
      Q=0.0
      ITYPE = 15
      CALL FREON (T2,PD,H ,S,Q,V ,ITYPE)
      IF(ITYPE.NE.0)  GO TO 98
      WRITE(-,010) T2
      STOP
98    CONTINUE
      Q=0.0
      ITYPE = 25
      CALL FREON (T,PD,HZ,S,Q,V,ITYPE)
```

```
117   RPDC=PD/PA
      IF (RPDC .GT. 1. .AND. RPDC .LT. 10.)  GO TO 118
      WRITE(-,618)
      IERR=1
      GO TO 501
118   VEFFDC=1.0235-7.5871E-02*RPDC+3.3267E-03*RPDC**2
      FF= MDOTDC*VB/VEFFDC
C      EXPANSION VALVE
      VEFFII=1.0235-7.5871E-02*RPII+3.3267E-03*RPII**2
      PII=PD/RPII
      ITYPE=25
      Q=1.0
      CALL FREON(T,PII,H,S,Q,V,ITYPE)
      TII=T+SHEAT
      ITYPE=12
      CALL FREON(TII,PII,HII,S,Q,VII,ITYPE)
      CVALVE=(FF*VEFFII/VII)/SQRT(PD-PII)
      COPII=(HC-HD)/(HII-HD)
C  CHECK THAT EXPANSION VALVE ISN'T WIDE OPEN AT DESIGN CONDITIONS
      IF(CVALVE*SQRT(PD-PA).GT.MDOTDC) GO TO 119
      WRITE(-,710)
710   FORMAT(' ****WARNING**** EXPANSION VALVE IS WIDE OPEN AT DESIGN
     1CONDITIONS')
119   CONTINUE
C  CNDNSR SIZING
      QRSH=MDOTDC*(HC-HY)
      QR2P=MDOTDC*(HY-HZ)
      CCRSH=QRSH/(TC-TY)
      CC2=M2DOTD*CP2
      UC2P=1./(1./HR2P+1./H2/ARCOND)
      UCSH=1./(1./HRSHD+1./H2/ARCOND)
      GO TO (130,120),ICHX
120   CONTINUE
C  SIZING OF CROSSFLOW CNDNSR (AIR)
C  SEE TLF ANALYSIS FOR CLARIFICATION
      ALPHA=UC2P/CC2
      BETA=QR2P/CC2/(TY-T2INDC)
      DELTA=UCSH/CC2
      SIGMA=CCRSH/CC2
      TAU=QRSH/CC2/(TC-T2INDC)
      THETA=-SIGMA*ALOG(1.-TAU/SIGMA)
      PHI=1.-THETA-BETA
      IF(PHI) 10,10,15
10    IERR=1
      WRITE(-,701)
701   FORMAT(' 1.-THETA-BETA IS NON POSITIVE')
      GO TO 501
15    CONTINUE
      IKCNT=0
      ART=0.
17    ART=ART+5.
      DFDA=-DELTA*(1.-BETA)*EXP(-DELTA*ART)-ALPHA*(1.-THETA)*
     1EXP(-ALPHA*ART)+(ALPHA+DELTA)*EXP(-(ALPHA+DELTA)*ART)
      IKCNT=IKCNT+1
      IF(IKCNT.GT.20) STOP
      IF(DFDA) 18,17,17
18    ART=ART+5.
```

```
      CE1=M1DOTD*CP1
      QA=MDOTDC*(HB-HD)
      EFFE=QA/CE1/(T1INDC-TA)
      IF(EFFE.LT.1.) GO TO 460
      WRITE(-,580)
      IERR=1
      GO TO 501
460   UAEVAP=-CE1*ALOG(1.-EFFE)
      UEVAP=1./(1./HBOILD+1./H1/AREVAP)
      AEVAP=UAEVAP/UEVAP
500   IF(IPRSZ.NE.1) GO TO 515
501   WRITE(-,-) PAR
      GO TO (520,522),IMODE
520   WRITE(-,530)
      GO TO 525
522   WRITE(-,631)
525   WRITE(-,632) (PAR(I),I=1,7),PAR(17)
      WRITE(-,620) PA,PD,HB,HC,HD
      WRITE(-,621) MDOTDC,RPDC,VEFFDC,FF
      WRITE(-,629) CVALVE
      GO TO (502,504),ICHX
502   WRITE(-,622)
      GO TO 505
504   WRITE(-,623)
505   WRITE(-,624) CC2,CCRSH,EFFCSH,EFFC2P,H2,HRSHD,HR2P,UCSH,UC2P
     1,ART,ARCOND,AF
510   WRITE(-,627) EFFE
512   WRITE(-,628) CE1,H1,HBOILD,UEVAP,AEVAP,AREVAP
      IF(IERR.EQ.1) STOP
515   RETURN
579   FORMAT(' EFFCSH GREATER THAN 1 IN HPSIZE')
580   FORMAT(' EFFE GREATER THAN 1 IN HPSIZE')
581   FORMAT(' EFFC2P IS GREATER THAN 1 IN HPSIZE')
585   FORMAT(' EFFSC GREATER THAN 1 IN HPSIZE')
586   FORMAT(' EFFCSH*(1.+CRCSH) IS GREATER THAN 1 IN HPSIZE')
587   FORMAT(' COND. GAMMA IS GREATER THAN 1 IN HPSIZE')
588   FORMAT(' SUBCLR GAMMA IS GREATER THAN 1 IN HPSIZE')
610   FORMAT(' FREON CALLED AT TZ=',F10.4)
611   FORMAT(' FREON CALLED AT PD=',F10.4)
612   FORMAT(' FREON CALLED AT TA=',F10.4,', HD=',F10.4)
613   FORMAT(' FREON CALLED AT PA=',F10.4)
614   FORMAT(' FREON CALLED AT TB=',F10.4,', PA=',F10.4)
615   FORMAT(' FREON CALLED AT PD=',F10.4,', S=',F10.4)
616   FORMAT(' FREON CALLED AT PD=',F10.4,' HC=',F10.4)
617   FORMAT(' FREON CALLED AT PD=',F10.4)
618   FORMAT(' DESIGN CONDITION RP IS NOT WITHIN RANGE OF 1 TO 10')
620   FORMAT(/' THE DESIGN CONDITION STATES ARE:'/
     1' PB=SUCTION PRESSURE=',F10.4/
     1' PC=DISCHARGE PRESSURE=',F10.4/
     1' HB=SUCTION ENTHALPY=',F10.4/
     1' HC=DISCHARGE ENTHALPY=',F10.4/
     1' HD=THROTTLING ENTHALPY=',F10.4)
621   FORMAT(/' COMPRESSOR DESIGN PARAMETERS:'/
     1' MDOTDC=MASS FLOW RATE=',F10.4/
     1' RPDC=PRESSURE RATIO=',F10.4/
     1' VEFFDC=VOLUMETRIC EFFICIENCY=',F10.4/
     1' FF=DISPLACEMENT RATE=',F10.4)
```

```
1       ICT=2
        CP1=PAR(2)
        CP2=PAR(3)
        ETAA=PAR(10)
        PMAX=PAR(11)
        ICHX=PAR(16)
        SHEAT=PAR(17)
        RPII=PAR(22)
        CFROST=PAR(23)
        IPR=PAR(29)
C  FIND THE INITIAL GUESS OF PRESSURE
2       ITYPE=15
        T=XIN(3)+PAR(19)
        CALL FREON(T,PC,H,S,1.,V,ITYPE)
        ITYPE=15
        T=XIN(1)-PAR(18)
        CALL FREON(T,PB,H,S,1.,V,ITYPE)
C  READ THE NEW INPUTS
5       T1IN=XIN(1)
        M1DOT=PAR(5)
        T2IN=XIN(3)
        M2DOT=PAR(7)
        ICNT1=0
        ICNT2=0
        ICNT3=0
C  LOCATE PT B
        Q=1.0
        ITYPE=25
        CALL FREON (T,PB,H,S,Q,V,ITYPE)
        IF(ITYPE.NE.0) GO TO 191
        WRITE(-,601) PB
        STOP
191     CONTINUE
        TB=T+SHEAT
        ITYPE=12
        CALL FREON (TB,PB,HB,SB,Q,VB,ITYPE)
        IF(ITYPE.NE.0) GO TO 199
        WRITE(-,602) TB,PB
        STOP
199     RP=PC/PB
        IF(RP.LT.12.) GO TO 200
        WRITE(-,801)  T1IN,T2IN
801     FORMAT(' RP IS OVER 12 AT ',2F10.4)
        GO TO 499
200     VEFF=1.0235-7.5871E-02*RP+3.3267E-03*RP**2
        MDOTR=FF*VEFF/VB
190     IPCOK=0
C  LOCATE PT C
        ITYPE = 24
        CALL FREON (T,PC,H,SB,Q,V,ITYPE)
        IF(ITYPE.NE.0) GO TO 201
        WRITE(-,603) PC,SB
        STOP
201     CONTINUE
        HC=(H-HB)/ETAA+HB
        ITYPE=23
        CALL FREON (TC,PC,HC,S,Q,V,ITYPE)
```

```
      STOP
  206 CONTINUE
      EPAR(1)=PB
      EPAR(2)=M1DOT
      EPAR(3)=MDOTR
      EPAR(4)=CP1
      EPAR(5)=CPLIQP
      CALL BOILER(IEVAP,EPAR,TA,HO,TB,HB,T1IN,T1OUT,QA)
      Q=1.0
      ITYPE=25
      CALL FREON(T,PB,H,S,Q,V,ITYPE)
      TBLINE=T+SHEAT
      ITYPE=12
      CALL FREON(TBLINE,PB,HBLINE,S,Q,V,ITYPE)
      DELHB1=HB-HBLINE
      IF(ICNT3.NE.0) GO TO 317
      IF(DELHB1.GT.-20..AND.DELHB1.LT.50.) GO TO 317
      ICNT3=1
      TA=T1IN-PAR(13)
      ITYPE=15
      CALL FREON(TA,PB,H,S,1.,V,ITYPE)
      ITYPE=12
      TB=TA+SHEAT
      CALL FREON(TB,PB,H,S,Q,VB,ITYPE)
      RP=PC/PB
      VEFF=1.0235-7.5871E-02*RP+3.3267E-03*RP**2
      MDOTR=FF*VEFF/VB
      GO TO 206
  317 IF(DELHB1.LT.2.) GO TO 318
      PBO=PB*(1.-PBINC1/PCRIT)
      GO TO 325
  318 IF(DELHB1.GT.EPS)  GO TO 320
      IF(DELHB1.LT.-EPS) GO TO 322
      IF(IPCCK.EQ.1) GO TO 400
  320 PBO=PB*(1.+PBINC2/PCRIT)
      GO TO 325
  322 PBO=PB*(1.-PBINC2/PCRIT)
  325 CONTINUE
C   LOCATE PT AO
C   FIRST DETERMINE APPROX VBO AT PBO TO GET NEW MDOTR
      Q=1.
      ITYPE=25
      CALL FREON(T,PBO,H,S,Q,V,ITYPE)
      TBO=T+SHEAT
      ITYPE=12
      CALL FREON(TBO,PBO,HBLINE,SBP,Q,VBO,ITYPE)
      RP=PC/PBO
      VEFF=1.0235-7.5871E-02*RP+3.3267E-03*RP**2
      MDOTR=FF*VEFF/VBO
  328 ITYPE=23
      CALL FREON(TAO,PBO,HO,S,Q,V,ITYPE)
      EPAR(1)=PBO
      EPAR(3)=MDOTR
      CALL BOILER(IEVAP,EPAR,TAO,HO,TBO,HBO,T1IN,T1OUT,QA)
      DELHBO=HBO-HBLINE
  330 DERIV2=(DELHBO-DELHB1)/(PBO-PB)
      PB=PB-DELHB1/DERIV2
```

```
      PC=PB
804   RP=PC/PB
      FLOW=CVALVE*SQRT(PC-PB)
      ITYPE=25
      Q=1.
      CALL FREON(T,PB,H,S,Q,V,ITYPE)
      TB=T+SHEAT
      ITYPE=12
      CALL FREON(TB,PB,HB,SB,Q,VB,ITYPE)
      VEFF=1.0235-7.5871E-02*RP+3.3267E-03*RP**2
      MDOTR=FF*VEFF/VB
      DIFF=MDOTR-FLOW
      IF(ABS(DIFF).LT.5.0) GO TO 820
      DERIV=(DIFFO-DIFF)/(PCO-PC)
      IF(IPR.EQ.1)  WRITE(-,805) LCNT,PC,PB,MDOTR,FLOW,DERIV
805   FORMAT(I5,5F12.4)
      DIFFO=DIFF
      PBO=PB
      PCO=PC
      LCNT=LCNT+1
      IF(LCNT.LT.20.) GO TO 800
      WRITE(-,810)
810   FORMAT(' LCNT EQUALS 20')
      STOP
820   ITYPE=24
      CALL FREON(T,PC,H,SB,Q,V,ITYPE)
      HC=HB+(H-HB)/ETAA
      Q=0.
      ITYPE=25
      CALL FREON(T,PC,HD,S,Q,V,ITYPE)
450   QR=MDOTR*(HC-HD)
      QA=MDOTR*(HB-HD)
C   EVAPORATOR FROST CHECK
      IF((T1IN+TA)/2..GT.32.) GO TO 500
      QDFRST=CFROST*QR
      QR=QR-QDFRST
      QA=QA-QDFRST
      GO TO 500
495   WRITE(-,620) T1IN,T2IN
       STOP
495   QR=0.0
      QA=0.0
601   FORMAT(' FREON CALLED AT PB=',F10.4)
602   FORMAT(' FREON CALLED AT TB=',F10.4,', PB=',F10.4)
603   FORMAT(' FREON CALLED AT PC=',F10.4,', SB=',F10.4)
604   FORMAT(' FREON CALLED AT PC=',F10.4,', HC=',F10.4)
605   FORMAT(' FREON CALLED AT PB=',F10.4,', HD=',F10.4)
620   FORMAT(' FAIL CONVERGE IN 12 ITERATIONS AT',2F9.4)
622   FORMAT(I4,3F8.2/1X,7F8.2)
500   RETURN
      END
```

A2.4 INTERP

```
      SUBROUTINE INTERP(T1IN,T2IN,QA,QR)
      DIMENSION QR33(3,3),QR3(3),QA33(3,3),QA3(3)
      COMMON/GRID/TLO,THI,DELT,N
```

```
7       XIN(1)=TLO+(L-1)*DELT
        CALL HTPMP(PAR,XIN,QA,QR)
9       QADD(L,J)=QA
        QREJ(L,J)=QR
10      CONTINUE
C  FILL UP REST OF ARRAY WITH LOWER DIAGONAL VALUES
        DO 15 J=1,N
        II=J+2
        DO 15 I=II,N
        QADD(I,J)=QADD(J+1,J)
15      QREJ(I,J)=QREJ(J+1,J)
        IF(ISAVE.EQ.0) RETURN
        DO 20  J=1,N
        DO 20  I=1,N
20      WRITE(ISAVE,-) QREJ(I,J),QADD(I,J)
        RETURN
30      ISAVE=-ISAVE
        DO 40  J=1,N
        DO 40  I=1,N
40      READ(ISAVE,-) QREJ(I,J),QADD(I,J)
        RETURN
        END
```

A2.6 BOILER

```
        SUBROUTINE BOILER(TEVAP,PAP,TCI,HCI,TCO,HCO,THI,THO,QA)
        DIMENSION PAR(7)
         REAL MDOTH,MDOTC,M1DOTD
        COMMON/EVAP/HBOILD,H1,AREVAP,AEVAP,M1DOTD,TDIF
        PMAX=PAR(1)
        MDOTH=PAR(2)
        MDOTC=PAR(3)
        CPH=PAR(4)
        CPC=PAR(5)
        AT=AEVAP
        CH=MDOTH*CPH
C   SIMPLIFIED MODEL IN WHICH NO SUPERHEAT HEAT EXCHANGER
C   EVER EXISTS. SINCE THE HEAT TRANSFERRED IN SUPERHEAT HEAT
C   EXCHANGER IS VERY SMALL IN A HEAT PUMP APPLICATION, ASSUME ALL HEAT
C   IS TRANSFERRED TO BOILING REFRIGERANT.
        HBOIL=HBOILD*(THI-TCI)/TDIF
        IF(HBOIL.LT.HBOILD/10.)  HBOIL=HBOILD/10.
        UO=1./(1./H1/AREVAP+1./HBOIL)
        E=1.-EXP(-UO*AT/CH)
        THO=THI-E*(THI-TCI)
        QA=CH*(THI-THO)
        HCO=HCI+QA/MDOTC
        ITYPE=23
        CALL FREON(TCO,PMAX,HCO,S,Q,V,ITYPE)
        RETURN
        END
```

```
      GO TO 315
300   CONTINUE
C  CROSS FLOW
C  C ON AIR SIDE DEPENDS ON AREA FRACTION ASSOCIATED WITH
C  DESUPERHEATING VAPOR (SEE TLF ANALYSIS)
C  A1 REDUCES TO SAME FORMULA NO MATTER WHICH SIDE HAS MAX C
C  THIS IS TRUE EVEN THOUGH E1 IS DIFFERENT FOR DIFFERENT CMAX
      E1=-Q1/(CH1*(THI-TCI))
      IF(E1.LT.1.0) GO TO 310
C  RETURN WITH A LARGE NEGATIVE DELHO
305   DELHO=HH3-HH2
      RETURN
310   GAMMA=1.-EXP(-USH*ART/(MDOTC*CPC))
      A1=(-CH1*ART/(MDOTC*CPC*GAMMA))*ALOG(1.-E1)
      IF(A1.GT.ART) GO TO 305
      A2=ART-A1
C  IN 2-PHASE  CMAX=CMIXED=INFINITY
      CC2=MDOTC*CPC*A2/ART
      E2=1.-EXP(-U2P*A2/CC2)
      TCO2=TCI+E2*(TH2-TCI)
      Q2=CC2*(TCI-TCO2)
315   HHO=HH2+Q2/MDOTH
      QR=Q1+Q2
      TCO=TCI-QR/(MDOTC*CPC)
      DELHO=HH3-HHO
      RETURN
601   FORMAT(' TH2 IS GREATER THAN THI IN CNDNSR')
      END
```

No.	Parameters	Description
21	IPRSZ	Option to printout sizing information computed in HPSIZE
22	RPII	Pressure ratio at which valve becomes fully open
23	CFROST	Percentage of air source evaporator capacity lost below freezing point
24	HR2P	Design condition condensing heat transfer coefficient
25	HRSHD	Design condition condenser de-superheating heat transfer coefficient
26	H2	Condenser exchange fluid side heat transfer coefficient
27	AREVAP	Evaporator exchange fluid to refrigerant area ratio
28	ARCOND	Condenser exchange fluid to refrigerant area ratio
29	IPR	Option to print out intermediate results during HTPMP solution
30	MODE	Heat pump control mode (1=control on temperatures, 2=control on heating rates)

13) Holladay, W.L., "Heat Transfer at Simulated Altitudes," Refrig. Eng., vol. 64, no. 5, p. 39 (May 1956).

14) Trane Air Conditioning Manual, Chapter VI, The Trane Company, LaCrosse, Wisconsin (1968).

15) Downing, R.C. and Knight, B.W., "Computer Program for Calculating Properties of the 'Freon' Refrigerants," 'Freon' Products Bulletin, RT-52, E.I. du Pont de Nemours and Co. (1971).

16) Bliss, R.W., "The Derivation of Several 'Plate-Efficiency Factors' Useful in the Design of Flat-Plate Solar Heat Collectors," Solar Energy, vol. 3, no. 4, pp. 55-64 (1959).

17) Liu, B.Y.H. and Jordan, R.C., "The Interrelationship and Characteristic Distribution of Direct, Diffuse and Total Solar Radiation," Solar Energy, vol. IV, pp. 1-19, (July 1960).

18) Ward, D.S. and Löf, G.O.G., paper presented at Fort Collins ISES meeting August 1974. "Design and Construction of a Residential Solar Heating and Cooling System."

19) Duffie, J.A. and Beckman, W.A., Solar Energy Thermal Processes, Wiley, New York, (1974)

20) Baker, M., Touloukian, T.S., & Hawkins, G.A. "Heat Transfer Film Coefficients for Refrigerants Boiling Inside Tubes", Refrig. Eng., vol. 61, no. 9, p. 986, (Sept. 1953).

21) Stoecker, W.F., "How Frost Formation on Coils Affects Refrigeration Systems", Refrig. Eng., vol. 65, no. 2, p. 42 (Feb. 1957).

22) Jaster, H., Corporate Research and Development, General Electric Co., Schenectady, N.Y., personal communication.

23) Carrier Heat Pump Systems - Form 38BQ-8P, Carrier Corp. (1974).

24) Stoecker, W.F., Refrigeration and Air Conditioning, McGraw-Hill, New York, (1958)

25) Klein, S.A., "A Design Procedure for Solar Heating Systems", paper to be presented at ISES annual meeting in Los Angeles (1975).

26) Whillier, A., "Design Factors Influencing Solar Collector Performance", Chapter III of Low Temperature Engineering Application of Solar Energy, ASHRAE, editor R.C. Jordan, (1967).

27) Bliss, R.W., "The derivation of Several Plate Efficiency Factors Useful in the Design of Flat-Plate Solar Heat Collectors", Solar Energy, vol. 3, no. 4, pp. 55-64 (1959).